U.G.A.M.P. INTERNAL REPORT

UK Universities Global Atmospheric Modelling Programme

UGAMP Internal Report No. 44a

The TOMCAT Offline Transport Model
Part I. Stratospheric Chemistry Code

Martyn Chipperfield

August 1996

This paper has not been published and is for internal circulation within UGAMP only.

The TOMCAT Offline Chemical Transport Model Part I. Stratospheric Chemistry Code

Martyn Chipperfield Centre For Atmospheric Science University of Cambridge.

August 1996

Version 1.0

Contents

1	Intr	roduction	3
2	The	e Chemical Scheme	4
	2.1	Coupled Short-Lived Species	4
		2.1.1 O_x Species	Ę
		2.1.2 NO_x Species	5
		2.1.3 ClO_x Species	5
		2.1.4 BrO _x Species	Ę
		2.1.5 HO_x Species	Ę
		2.1.6 CH_yO_x Species	
	2.2	Short-Lived Species in Equilibrium	8
	2.3	Long-Lived Species	
	2.4	Fixed Species	S
3	Che	emical Integration	10
	3.1	Semi-Implicit Symmetric Method	10
		3.1.1 Formulation of Matrix M	
	3.2	UGAMP Scheme	11
	3.3	NCAR Implicit Scheme	
	3.4	Fourth Order Runge Kutta Scheme	
	3.5	Simple Forward Euler Scheme	
	3.6	Chemical Timestep	
4	Pho	otolysis Rate Calculation	12
	4.1	BrCl	13
	4.2	CH ₄	13
	4.3	$\mathrm{H}_2\mathrm{O}$	
	4.4	NO	13
	4.5	O_2	13
	4.6	$\stackrel{-}{\mathrm{O}_3}$	13
	4.7	OCIO	
5	Neg	gative Species Concentrations	14

6	Heterogeneous Chemistry	14
	6.1 Liquid Aerosols	
	6.2 Sulphuric Acid Tetrahydrate	 16
	6.3 Nitric Acid Trihydrate	 16
	6.4 Ice Particles	 17
7	Using The TOMCAT Chemical Scheme	17
•	7.1 Common Decks	
	7.2 Subroutines	
	7.3 Fortran Channels	
	7.4 Photolysis Tables	
	7.5 Chemical Integration Scheme	
	7.6 Heterogeneous Chemistry	
	7.7 Inlined Subroutines	
	7.8 Interface With Chemical Scheme	
8	Tests	20
	8.1 Compiler Tests	20
	8.2 Box Model Tests	
	8.2.1 Integration Scheme	
	8.2.2 Use of Families	
	8.3 Photolysis Rates	
	8.4 Heterogeneous Chemistry	
	8.5 Coupling to 2D Transport Model	
	8.6 Domain Filling Trajectories	
	8.7 3D Transport Model	 22
9	Summary	31
10	Acknowledgements	31
		-
11	Appendix 1. Photochemical Reactions.	33
12	Appendix 2. U.S. Standard Atmosphere.	37
13	Appendix 3. CH ₄ Oxidation Scheme.	38
14	Appendix 4. Cray Flowtrace.	39

1 Introduction

This report describes the TOMCAT stratospheric chemistry scheme. The chemical scheme contains a fairly detailed description of stratospheric chemistry, including heterogeneous reactions on polar stratospheric clouds (PSCs) and liquid sulphate aerosols. The model is written to be computationally efficient for use in three-dimensional (3D) atmospheric models on vector machines such as a Cray. However, the chemical model can also be used as a box model, coupled to a 2D latitude-height model, or in any other configuration.

I originally developed this chemical model at Météo-France in Toulouse during 1991/92. The original requirement was to include only short-lived radical and reservoir species for short 3D model runs of around one week. Since this time, 3D chemical models have become more established and are now integrated for seasonal simulations. Accordingly, the the chemical scheme has been modified gradually (e.g. to include long-lived species such as N_2O) to permit these longer integrations. This report is an attempt to document a new standard version of the TOMCAT stratospheric chemistry code which is suitable for multi-year simulations. For example, the 3D chemistry scheme described here now contains all of the long-lived source gases and reactions

included in the standard Edinburgh/Cambridge 2D model [e.g. Kinnersley, 1996]. However, the code is still computationally efficient to run.

This report is Part I of a series of three reports describing the TOMCAT off-line chemical transport model (CTM). Part II [Chipperfield and Simon, 1996] deals with the basic dynamical part of the CTM and part III [Stockwell and Chipperfield, 1996] describes the parameterisations of convection and vertical diffusion in the troposphere.

2 The Chemical Scheme

The simplest approach to writing a stratospheric chemistry model is to integrate all chemical species separately with no assumption of photochemical equilibrium. However, this is completely impractical in a 3D model. For the scheme described here I decided to combine short-lived species together into families where possible. Even if one was to integrate chemical species separately within a box, it does not seem realistic to transport such closely coupled (and short-lived) species as Cl and ClO individually. Another good reason for employing the family approach is to save CPU time and memory. If species are grouped together into families one reduces the number of advected tracers. In addition, one of the most costly subroutines in the standard model is that which inverts the matrix for the SIS method (see below). The number of calculations performed in inverting a NxN matrix (with the Gaussian elimination method as used in the subroutine MATRIX) is proportional to N³. Therefore, even allowing for the fact that the model runs on a vectorised machine, if the number of chemical species (or families) in the matrix is reduced from say 20 to 14 by the use of families the time taken to solve the chemical equations by the SIS method is roughly halved. A problem with grouping species together in families is how to partition them at night when photochemical equilibrium may no longer apply. For example, the species OCIO has a very short lifetime during the day but at night it is not destroyed. Thus, it is not simple to include this in, say, a ClO_x family. With these considerations in mind the following families were chosen for the model chemistry scheme: $O_x = O(^3P) + O(^1D) + O_3$, $NO_x = N + NO + NO_2$, $CO_x = CI + CIO + 2CI_2O_2$ and BrO_x (=Br + BrO). These species establish a rapid equilibrium with each other and the partitioning can be calculated at night. Table 1 lists the species contained in the model.

Coupled short	$O_x (= O_3 + O(^3P) + O(^1D)), H_2O_2$
lived species	$NO_x (= N + NO + NO_2), NO_3, N_2O_5, HNO_3, HO_2NO_2,$
	ClO_x (=Cl + ClO + 2Cl ₂ O ₂), ClONO ₂ , HCl, HOCl, OClO,
	BrO_x (=Br + BrO), $BrONO_2$, $BrCl$, HBr , $HOBr$
Steady state	$H, OH, HO_2,$
	$\mathrm{CH_{3},CH_{3}O_{2},CH_{3}O,CH_{2}O,HCO,CH_{3}OOH}$
Source gases	CH ₄ , N ₂ O, CO, H ₂ O, CFCl ₃ (F11), CF ₂ Cl ₂ (F12),
and long-lived	CHF_2Cl (F22), $C_2F_3Cl_3$ (F113), CH_3Cl , CH_3CCl_3 , CCl_4 ,
species	CH ₃ Br, CBrClF ₂ , CBrF ₃ ,
	COF ₂ , COFCl, HF,
Fixed	O_2 , N_2 , H_2

Table 1. Chemical species contained in the model

Appendix 1 lists the photochemical reactions used in the model. The photochemical data is, in general, taken from NASA/JPL [1994].

2.1 Coupled Short-Lived Species

When using a family approach great care must be taken in formulating the expressions which partition members within a family. As well as the reactions which directly interconvert family members, it is very important to also include terms for reaction paths which indirectly interconvert species. These indirect routes in e.g. the ratio [Cl]/[ClO] are often associated with catalytic O_3 loss cycles.

2.1.1 O_x Species

The partitioning between members of the odd-oxygen O_x family $(=O(^1D) + O(^3P))$ is calculated from:

$$\frac{[O(^{1}D)]}{[O_{3}]} = \frac{J_{O3a}}{k_{6a}[O_{2}] + k_{6b}[N_{2}]}$$
$$\frac{[O(^{3}P)]}{[O_{3}]} = \frac{J_{O3a} + J_{O3b}}{k_{2}[O_{2}][M]}$$

2.1.2 NO_x Species

The partitioning between members of the NO_x family (=N + NO + NO₂) is calculated from:

$$\frac{[N]}{[NO]} = \frac{J_{NO}}{k_{71}[O_2] + k_{72}[O_3]}$$

$$\frac{[NO]}{[NO_2]} = \frac{J_{NO2} + k_{16}[O] + J_{NO3a} \frac{[NO_3]}{[NO_2]}}{k_{17}[O_3] + k_{35}[HO_2] + k_{55}[ClO] + k_{101}[CH_3O_2] + k_{123}[BrO]}$$

where

$$\frac{[NO_3]}{[NO_2]} = \frac{k_{18}[O_3] + k_{20}[OH] \frac{[HONO_3]}{[NO_2]} + (J_{CNIT} + k_{63}[O]) \frac{[ClONO_2]}{[NO_2]} + J_{BNIT} \frac{[BrONO_2]}{[NO_2]} + (k_{92}[M] + J_{N2O5}) \frac{[N_2O_5]}{[NO_2]}}{J_{NO3a} + J_{NO3b} + k_{91}[NO_2][M]}$$

During the night, all of the NO_x is therefore in the form of NO_2 .

2.1.3 ClO_x Species

The partitioning between members of the ClO_x family (= $Cl + ClO + 2Cl_2O_2$) is calculated from:

$$\frac{[Cl]}{[ClO]} = \frac{k_{51}[O] + k_{55}[NO] + (2k_{68b} + k_{68c})[ClO] + k_{75a}[OH] + k_{114}[CH_3O_2] + k_{126}[BrO] + 2J_{Cl2O2} \frac{[Cl_2O_2]}{[ClO]} + J_{BrCl} \frac{[BrCl]}{[ClO]} + J_{HOCl} \frac{[HOCl]}{[ClO]} + J_{CNIT} \frac{[ClONO_2]}{[ClO]}}{k_{50}[O_3] + k_{59b}[HO_2] + k_{64b}[HOCl]} \\ \frac{[Cl_2O_2]}{[ClO]} = \frac{k_{68}[ClO][M]}{k_{69}[M] + J_{Cl2O2}}$$

2.1.4 BrO_x Species

The partitioning between members of the BrO_x family (=Br + BrO) is calculated from:

$$\frac{[Br]}{[BrO]} = \frac{k_{121}[O] + k_{123}[NO] + k_{124}[OH] + 2k_{127}[BrO] + (k_{125} + k_{126})[ClO] + J_{BrO} + J_{BRCl}\frac{[BrCl]}{[BrO]} + J_{HOBR}\frac{[HOBr]}{[BrO]} + J_{BRNO3}\frac{[BrONO_2]}{[BrO]}}{k_{120}[O_3]}$$

2.1.5 HO_x Species

The photochemical lifetimes of the HO_x species are very short throughout the stratosphere, typically less than 30 minutes. This is much shorter than dynamical timescales and so the abundance of the HO_x species will not depend directly on transport. In the model, therefore, H, OH and HO_2 are not integrated. Their abundances are derived by putting them in steady state. The concentration of species in the HO_x family (H, OH, HO_2) is calculated as follows (in the subroutine CRATIO). The 3 species are individually put into photochemical steady state giving the following expressions:

$$\frac{d[H]}{dt} = k_8[O][OH] + k_{32}[O(^1D)][H_2] + k_{34}[OH][CO]$$

$$+k_{58}[Cl][H_2] + k_{109}[OH][H_2] + J_{CH2Oa}[CH_2O]$$

$$+J_{HCl}[HCl] + J_{CH4}[CH_4] + J_{H2O}[H_2O]$$

$$-k_9[H][O_2] - k_{12}[H][O_3] - (k_{15a} + k_{15b} + k_{15c})[H][HO_2] = 0$$

$$\frac{d[OH]}{dt} = 2k_{7}[O(^{1}D)][H_{2}O] + k_{10}[O][HO_{2}]$$

$$+k_{12}[H][O_{3}] + 2k_{15a}[H][HO_{2}] + k_{31}[CH_{4}][O(^{1}D)] + k_{32}[O(^{1}D)][H_{2}]$$

$$+k_{35}[HO_{2}][NO] + k_{36}[HO_{2}][O_{3}] + k_{59b}[Cl][HO_{2}]$$

$$+k_{67}[HOCl][O] + k_{107}[CH_{2}O][O] + k_{131}[HOBr][O]$$

$$+J_{HNO_{3}}[HNO_{3}] + J_{HOCl}[HOCl] + 2J_{H2O_{2}}[H_{2}O_{2}]$$

$$+J_{HOBr}[HOBr] + J_{MHP}[CH_{3}OOH] + J_{H2O}[H_{2}O]$$

$$-k_{8}[OH][O] - k_{11}[OH][O_{3}] - k_{13}[OH][HO_{2}]$$

$$-2k_{14}[OH][OH] - k_{20}[OH][HNO_{3}] - k_{21}[OH][NO_{2}][M]$$

$$-k_{26}[OH][H_{2}O_{2}] - k_{30}[OH][CH_{4}] - k_{34}[CO][OH]$$

$$-k_{40}[HO_{2}NO_{2}][OH] - k_{60}[OH][HCl] - k_{66}[HOCl][OH]$$

$$-(k_{75a} + k_{75b})[OH][ClO] - k_{104}[OH][CH_{3}OOH] - k_{106}[OH][CH_{2}O]$$

$$-k_{109}[OH][H_{2}] - k_{124}[OH][BrO] - k_{136}[OH][HBr]$$

$$= 0$$

$$\begin{split} \frac{d[HO_2]}{dt} &= k_9[H][O_2] + k_{11}[OH][O_3] \\ + k_{26}[OH][H_2O_2] + k_{39}[HO_2NO_2][M] + k_{52}[H_2O_2][Cl] \\ + k_{75a}[ClO][OH] + k_{105}[CH_3O][O_2] + k_{108}[HCO][O_2] \\ + k_{124}[OH][BrO] + J_{PNA}[HO_2NO_2] \\ - k_{10}[O][HO_2] - k_{13}[OH][HO_2] - (k_{15a} + k_{15b} + k_{15c})[H][HO_2] - 2k_{24}[HO_2][HO_2] \\ - k_{35}[NO][HO_2][M] - k_{36}[HO_2][O_3] - k_{37}[HO_2][NO_2][M] \\ - (k_{59} + k_{59b})[HO_2][Cl] - (k_{65} + k_{65b})[ClO][HO_2] \\ - k_{102}[CH_3O_2][HO_2] - (k_{130} + k_{130b})[BrO][HO_2] \\ - k_{135}[Br][HO_2] \\ = 0 \end{split}$$

This gives three quadratic equations that can be solved. As the three HO_x species are highly coupled this is done *iteratively* until a solution is reached. To speed up the convergence of this iterative loop, an initial guess of the partitioning of species in the HO_x family is calculated from:

$$\frac{[H]}{[OH]} = \frac{k_8[O] + k_{34}[CO] + k_{109}[H_2]}{k_{12}[O_3] + k_9[O_2][M]}$$

$$\frac{[HO_2]}{[OH]} = \frac{k_9[O_2][M] \frac{[H]}{[OH]} + k_{11}[O_3] + k_{26}[H_2O_2] + k_{75a}[ClO] + k_{124}[BrO]}{k_{10}[O] + k_{35}[NO] + k_{36}[O_3]}$$

and the total abundance of HO_x is calculated from:

$$\frac{d[HO_x]}{dt} = 2k_7[O(^1D)][H_2O] + k_{31}[O(^1D)][CH_4]$$
$$+2k_{32}[O(^1D)][H_2] + k_{39}[HO_2NO_2][M]$$
$$+k_{67}[HOCl][O] + J_{HNO3}[HNO_3] + J_{PNA}[HO_2NO_2]$$

$$\begin{split} +J_{HOCl}[HOCl] + 2J_{H2O2}[H_2O_2] + J_{HCL} \\ +J_{HOBr}[HOBr] + J_{CH4}[CH_4] + 2J_{H2O}[H_2O] \\ +J_{C2OA}[CH_2O] + J_{MHP}[CH_3OOH] \\ -2k_{13}[OH][HO_2] - 2k_{14}[OH][OH] \\ -2(k_{15b} + k_{15c})[H][HO_2] - 2k_{24}[HO_2][HO_2] \\ -k_{20}[OH][HNO_3] - k_{21}[OH][NO_2][M] - k_{30}[OH][CH_4] \\ -k_{37}[HO_2][NO_2][M] - k_{40}[HO_2NO_2][OH] \\ -k_{59}[Cl][HO_2] - k_{60}[OH][HCl] - k_{65}[ClO][HO_2] \\ -k_{66}[HOCl][OH] = 0 \end{split}$$

By substituting for HO_2 and H a quadratic equation is obtained which can be solved to determine the initial estimate of OH.

2.1.6 CH_yO_x Species

Details of the model's methane oxidation scheme are given in Appendix 3. The products of methane oxidation are put into steady state using the following expressions:

$$\frac{d[CH_3]}{dt} = k_{30}[OH][CH_4] + k_{31}[O(^1D)][CH_4] + k_{57}[Cl][CH_4] + J_{CH_4}[CH_4] - k_{100}[O_2][CH_3][M] = 0$$

$$\frac{d[CH_3O_2]}{dt} = k_{30}[OH][CH_4] + k_{31}[O(^1D)][CH_4] + k_{57}[Cl][CH_4] + k_{104}[OH][CH_3OOH] - k_{101}[NO][CH_3O_2] - k_{102}[HO_2][CH_3O_2] - k_{103}[CH_3O_2][CH_3O_2] - k_{114}[ClO][CH_3O_2] = 0$$

$$\frac{d[CH_3OOH]}{dt} = k_{102}[HO_2][CH_3O_2]$$

$$-(k_{104} + k_{115})[OH][CH_3OOH] - J_{MHP}[CH_3OOH] = 0$$

$$\frac{d[CH_3O]}{dt} = k_{30}[OH][CH_4] + k_{31}[O(^1D)][CH_4] + k_{57}[Cl][CH_4] - k_{105}[O_2][CH_3O] = 0$$

$$\frac{d[CH_2O]}{dt} = k_{30}[OH][CH_4] + k_{31}[O(^1D)][CH_4] + k_{57}[Cl][CH_4] + k_{111}[O(^1D)][CH_4] - k_{106}[OH][CH_2O] - k_{107}[O][CH_2O] - k_{110}[Cl][CH_2O] - k_{134}[Br][CH_2O] - (J_{CH_2OA} + J_{CH_2OB})[CH_2O] = 0$$

$$\begin{split} \frac{d[HCO]}{dt} &= J_{C2OA}[CH_2O] + k_{106}[OH][CH_2O] \\ + k_{107}[O][CH_2O] + k_{110}[Cl][CH_2O] - k_{108}[HCO][O_2] &= 0 \end{split}$$

These expressions are generally good approximations, except for $\mathrm{CH_2O}$ which has a lifetime of around 1 day in the lower stratosphere.

2.2 Short-Lived Species in Equilibrium

In the model the short-lived species OClO, BrCl and NO₃ are integrated separately as it is important to calculate accurately the abundance of these species at twilight and at night. However, during the daytime these species are rapidly photolysed and in photochemical equilibrium with the other ClO_x , NO_x and BrO_x species. Within the code these three species can be placed in photochemical equilibrium during the daytime by setting the parameter LEQM in SWITCH to TRUE. This will reduce the stiffness of the system and enable longer timesteps to be taken. Generally the UGAMP integration scheme needs LEQM to be TRUE while the defaults SIS scheme does not.

When in photochemical equilibrium the abundance of OClO, BrCl and NO₃ are calculated from:

$$\frac{[OClO]}{[ClO]} = \frac{k_{68C}[ClO] + k_{125}[BrO]}{J_{OClO}}$$

$$\frac{[BrCl]}{[BrO]} = \frac{k_{144}[ClO]}{J_{BrCl}}$$

$$\frac{[NO_3]}{[NO_2]} = \frac{k_{18}[O_3] + J_{CNIT} \frac{[ClONO_2]}{[NO_2]} + (k_{92}[M] + J_{N2O5}) \frac{[N_2O_5]}{[NO_2]}}{J_{NO3a} + J_{NO3b} + k_{91}[M][NO_2]}$$

2.3 Long-Lived Species

The source gases and long-lived species listed in table 1 are integrated according to the following continuity equations:

$$\frac{d[N_2O]}{dt} = -((k_{22} + k_{22b})[O(^1D)] + J_{N2O})[N_2O]$$

$$\frac{d[CH_4]}{dt} = -(k_{30}[OH] + k_{31}[O(^1D)] + k_{57}[Cl] + k_{111}[O(^1D)] + J_{CH4})[CH_4]$$

$$\frac{d[CO]}{dt} = k_{108}[HCO][O_2] + J_{C2OB}[CH_2O] - k_{34}[OH][CO]$$

$$\frac{d[CFCl_3]}{dt} = -(k_{48}[O(^1D)] + J_{F11})[CFCl_3]$$

$$\frac{d[CF_2Cl_2]}{dt} = -(k_{49}[O(^1D)] + J_{F12})[CF_2Cl_2]$$

$$\frac{d[CH_3Cl]}{dt} = -(k_{84}[OH] + k_{83}[O(^1D)] + J_{CH3CL})[CH_3Cl]$$

$$\frac{d[CH_3CCl_3]}{dt} = -(k_{82}[OH] + k_{81}[O(^1D)] + J_{MCFM})[CH_3CCl_3]$$

$$\frac{d[CCl_4]}{dt} = -(k_{80}[O(^1D)] + J_{CCL4})[CCl_4]$$

$$\frac{d[CHF_2Cl]}{dt} = -(k_{80}[OH] + k_{85}[O(^1D)] + J_{F22})[CHClF_2]$$

$$\frac{d[C_2F_3Cl_3]}{dt} = -(k_{87}[O(^1D)] + J_{F113})[C_2F_3Cl_3]$$

$$\frac{d[CH_3Br]}{dt} = -(k_{142}[OH] + k_{143}[O(^1D)] + J_{CH3BR})[CH_3Br]$$

$$\frac{d[CBrClF_2]}{dt} = -(k_{148}[O(^1D)] + J_{F1211})[CBrClF_2]$$

$$\frac{d[CBrClF_2]}{dt} = -(k_{140}[O(^1D)] + J_{F1301})[CBrF_3]$$

$$\frac{d[COF_2]}{dt} = -\frac{d[CF_2Cl_2]}{dt} - \frac{d[CHF_2Cl]}{dt} - \frac{d[CBrClF_2]}{dt} - \frac{d[CBrF_3]}{dt} - (k_{180}[O(^1D)] + J_{COF_2})[COF_2]$$

$$\frac{d[COFCl]}{dt} = -\frac{d[CFCl_3]}{dt} - \frac{d[C_2F_3Cl_3]}{dt} - (k_{181}[O(^1D)] + J_{COFCL})[COFCl]$$

$$\frac{d[HF]}{dt} = -\frac{d[CBrF_3]}{dt} + (k_{181}[O(^1D)] + J_{COFCL})[COFCl] + 2(k_{180}[O(^1D)] + J_{COF_2})[COF_2] - k_{61}[HF]$$

2.4 Fixed Species

The fixed species have the following volume mixing ratios:

Species	Mixing Ratio
N_2	0.791
O_2	0.209
H_2	0.5×10^{-6}

Table 2. Volume mixing ratios of fixed species.

3 Chemical Integration

All photochemical models rely on a numerical scheme to integrate the chemical continuity equations. It should be remembered that all such schemes will be subject to some degree of numerical errors. Accurate integration schemes are available but these will be computationally expensive. Cheaper integration schemes are usually less accurate and/or less stable. Some implicit schemes may be stable but not accurate. I have included four different integrations schemes in the TOMCAT model to intercompare them and find the most suitable scheme for use in a 3D model. They are described below:

3.1 Semi-Implicit Symmetric Method

Ramaroson [1989] developed a method for integrating the stiff set of chemical continuity equations which is referred to as the 'semi-implicit symmetric' (SIS) method. This is the default integration scheme for TOMCAT and is described here.

The chemical continuity equation for a species i with concentration n_i is written:

$$\frac{dn_i}{dt} = P_i - L_i n_i = Q_i$$

This can be written in a vector form for a range of N species, $\overline{n} = n_1, n_2, ... n_N$

$$\frac{d\overline{n}}{dt} = \overline{Q}(t, \overline{n}(t))$$

Ramaroson et al. [1992] described the development of this equation to form:

$$\overline{n}_{t+\Delta t} - \overline{n}_t = \frac{\Delta t}{2} \left[\overline{Q}(t, \overline{n}(t)) + \overline{Q}(t + \Delta t, \overline{n}(t + \Delta t)) \right]$$

In the SIS method this is solved by expanding $\overline{Q}(t + \Delta t, \overline{n}(t + \Delta t))$ in a Taylor series and rearranging to get

$$\overline{n}_{t+\Delta t} = \overline{n}_t + \frac{\Delta t}{2} \mathbf{J_t} \overline{n}_{t+\Delta t}$$

where \mathbf{J}_t is the Jacobian matrix

$$\mathbf{J_t} = \begin{pmatrix} \frac{\partial Q_1}{\partial n_1} & \frac{\partial Q_1}{\partial n_2} & \dots & \frac{\partial Q_1}{\partial n_N} \\ \frac{\partial Q_2}{\partial n_1} & \frac{\partial Q_2}{\partial n_2} & \dots & \frac{\partial Q_2}{\partial n_N} \\ \dots & \dots & \dots & \dots \\ \frac{\partial Q_N}{\partial n_1} & \frac{\partial Q_N}{\partial n_2} & \dots & \frac{\partial Q_N}{\partial n_N} \end{pmatrix}$$

Therefore to derive the concentrations at time $t + \Delta t$ it is a question of inverting the matrix

$$\mathbf{M} = \mathbf{I} - \frac{\Delta t}{2} \mathbf{J_t}$$

The SIS method has the desired properties of an integration scheme: it is accurate, stable and relatively fast compared to other methods for solving stiff systems.

3.1.1 Formulation of Matrix M

The method of integrating the chemical continuity equations with the SIS method means that modifications to the chemical scheme require a modification of the matrix \mathbf{M} . The form of the matrix means that a given reaction can appear in several continuity equations and so in several matrix elements. Therefore this section explains how to formulate the matrix \mathbf{M} and how to take account of species which are contained in chemical families.

Consider the reaction in which both reactants are integrated:

$$ClO + NO_2 + M \rightarrow ClONO_2 + M$$

Using the SIS method the change in ClO due to this reaction is given by:

$$[ClO]_{t+\Delta t} - [ClO]_t = \frac{\Delta t}{2} k_{62}[M]([ClO]_t[NO_2]_{t+\Delta t} + [ClO]_{t+\Delta t}[NO_2]_t)$$

Reaction (62) appears in the continuity equations for ClO, NO₂ and ClONO₂. As the two reactant molecules are both integrated it will appear in 6 elements of the Jacobian matrix J_m such as:

$$\frac{\partial Q_{ClO}}{\partial [NO_2]} = -k_{62}[M][ClO]$$

For the reasons mentioned above the TOMCAT model uses chemical families. This will change the format of the matrix \mathbf{M} . Now, if ClO is in the ClO_x family and NO₂ is in the NO_x family the change to ClO_x due to reaction (62) over 1 timestep will be written as:

$$[ClO_x]_{t+\Delta t} - [ClO_x]_t = \frac{\Delta t}{2} k_{62}[M]RCLO.RNO2([ClO_x]_t[NO_x]_{t+\Delta t} + [ClO_x]_{t+\Delta t}[NO_x]_t)$$

where RCLO is the ratio of [ClO]: $[ClO_x]$ and RNO2 is the ratio of $[NO_2]$: $[NO_x]$. Ramaroson [1989] and Ramaroson et al. [1992] described a 'fix' to avoid oscillations in very short-lived (e.g. Cl) species at sunrise and sunset. This consists of treating certain reactions involving these species (e.g. reaction (50)) fully implicitly with one species (e.g. O_3) assumed constant over the timestep. This approach is no longer necessary with the scheme described here as these short-lived species have been incorporated into families. Thus, all reactions involving two integrated species are treated semi-implicitly.

For a reaction involving only one reactant, or the reaction of an integrated species with a non-integrated species Ramaroson et al. [1992] described how these could be treated fully implicitly. For example for the reactions:

$$NO_2 + h\nu \rightarrow NO + O$$

 $NO_2 + OH + M \rightarrow HNO_3 + M$

The change to NO₂ due to these two reactions (if NO₂ is integrated) is given by:

$$[NO_2]_{t+\Delta t} - [NO_2]_t = -\Delta t (J_{NO2}[NO_2]_{t+\Delta t} + k_{21}[OH][M][NO_2]_{t+\Delta t})$$

Unfortunately, this reduces the accuracy of the SIS scheme. This seems to be most serious for fast photolysis reactions which produce odd oxygen. For example, the photolysis of NO_2 simply interconverts NO and NO_2 within the NO_x family but in terms of odd oxygen it is a rapid step in a many null cycles and must balance the other terms in these cycles. Therefore, in TOMCAT the photolysis reactions leading to odd oxygen production are also treated with the SIS method in the odd oxygen continuity equation.

3.2 UGAMP Scheme

The UGAMP integration scheme is described by Stott and Harwood [1993]. It is designed to be computationally efficient for use in 3D chemical models. It is a Euler backwards scheme in which an initial estimate of the solution is used as the first approximation in a Newton-Raphson iteration to the fully implicit solution. In the initial estimate, and in each iteration, a matrix inversion is avoided by approximating the matrix by its diagonal.

The number of iterations required is typically 10-15 for the chemical species used in TOMCAT. The number of iterations is controlled by the variable NRSTEPS in the subroutine ODEIMP.

3.3 NCAR Implicit Scheme

This simple implicit scheme integrates the chemical concentration from:

$$n_{t+\Delta t} = \frac{n_t + \Delta t P_i}{1 - \Delta t L_i}$$

with P_i and L_i evaluated at time t. This scheme does not necessarily conserve. As I have not included code to force conservation with this scheme its use is not recommended.

3.4 Fourth Order Runge Kutta Scheme

This is an accurate, but expensive, integration scheme which can be used as standard with which to compare the cheaper schemes. The cost of this scheme precludes its use in 3D experiments.

This scheme is commonly used in many fields. The differential equations are solved by:

$$n_{t+\Delta t} = n_t + \frac{k_1}{6} + \frac{k_2}{3} + \frac{k_3}{3} + \frac{k_4}{6} + O(\Delta t^2)$$

where

$$k_1 = \Delta t Q(t, n_t)$$

$$k_2 = \Delta t Q(t + \frac{\Delta t}{2}, n_t + \frac{k_1}{2})$$

$$k_3 = \Delta t Q(t + \frac{\Delta t}{2}, n_t + \frac{k_2}{2})$$

$$k_4 = \Delta t Q(t + \Delta t, n_t + k_3)$$

This was coded into TOMCAT using basic subroutines from Numerical Recipes [1990] which include an adaptive stepsize control.

3.5 Simple Forward Euler Scheme

Probably the simplest integration scheme is a simple forward Euler scheme. The chemical continuity equation for a species i, with concentration n_i , is written:

$$\frac{dn_i}{dt} = P_i - L_i n_i$$

$$n_{t+\Delta t} = n_t + \Delta t \left(\frac{dn}{dt}\right)_t$$

Although this scheme is unstable for short-lived species, it is fine for integrating very long-lived species (such as the tropospheric source gases) throughout the lower and middle atmosphere.

3.6 Chemical Timestep

When using a 3D model it is tempting to use a chemical timestep as large as possible in order to save computer time. However this can be dangerous as a long timestep will not enable the model to correctly resolve the diurnal cycle of the chemical species. Also, the longer the timestep the larger the possibility that the model will produce negative species concentrations which will need to be corrected introducing additional errors. The basic chemical timestep used in the model described here is 15 minutes. In tests this was the largest timestep which adequately coped with the above problems. Although integration schemes can be stable for longer timesteps the results are not necessarily accurate. I would recommend 30 minutes as the maximum timestep, with 15 minutes being preferred.

4 Photolysis Rate Calculation

The photolysis rates (J values) are calculated using a scheme based on Lary and Pyle [1991] and Lary [1991], which in turn was based on Meier et al. [1982] and Nicolet et al. [1982]. The scheme uses a four-dimensional look-up table (which has coordinates of pressure altitude, temperature, O_3 column and zenith angle) to interpolate precomputed J values to a particular location and time in the atmosphere. The scheme takes account of multiple scattering and spherical geometry and can calculate photolysis rates for zenith angles up to 96° , which

is important for applications to the polar lower stratosphere. Despite the fact that the look up table method is quite efficient the calculation of the photolysis rates is one of the most expensive calculations in the model. Therefore the J values are generally calculated once every 30 minutes during the middle of the day, when the cosine of the zenith angle changes quite slowly, and once every 15 minutes at sunrise and sunset.

The photochemical data used for the calculating the J rates are generally taken from NASA/JPL [1994]. Exceptions to this are listed here:

4.1 BrCl

The absorption cross sections of BrCl are calculated (in subroutine ACSBRCL) following the measurements and parameterisation of Maric et al. [1994]. The upper wavelength limit for this calculation is set to 517 nm, which should correspond to the limit for direct dissociation of the BrCl bond.

4.2 CH₄

The only contribution to the photolysis rate of CH_4 comes from the Lyman α line and is parameterised (in subroutine LYMANA) following Nicolet [see Brasseur and Solomon, 1984]:

$$J_{CH4} = 1.37 \times 10^{-17} \times 0.85 \times q_{\infty} e^{(-4.17 \times 10^{-19}.(N^{0.917}))}$$

where N is total O_2 column and q_{∞} is the flux at 121.6 nm at the top of the atmosphere.

4.3 H₂O

The photolysis of H_2O in the Lyman α line is parameterised (in subroutine LYMANA) following Nicolet [see Brasseur and Solomon, 1984]:

$$J_{H2O} = 1.40 \times 10^{-17} \times 0.85 \times q_{\infty} e^{(-4.17 \times 10^{-19}.(N^{0.917}))}$$

4.4 NO

The parameterisation of J_{NO} (implemented in the subroutine ACSNO) is based on Allen and Frederick [1982].

4.5 O_2

The photolysis of O_2 in the Lyman α line is parameterised (in subroutine LYMANA) following Nicolet [see Brasseur and Solomon, 1984]:

$$J_2 = (4.17 \times 10^{-19}.N^{0.083}) \times q_{\infty}.e^{(-4.17 \times 10^{-19}(N^{0.917}))}$$

4.6 O_3

The quantum yield of $O(^1D)$ from O_3 photolysis is parameterised (in subroutine QUANTO12) from Michelsen et al. [1994].

4.7 OClO

The model uses the 204 K data of Wahner et al. [1987]. The high resolution data was obtained [A. Wahner personal communication, 1996] and averaged onto the model wavelength grid.

5 Negative Species Concentrations

Negative concentrations of chemical species are unrealistic and when then occur in the model they must be corrected. Negatives can be caused either as a result of the chemical integration or as a result of the model transport scheme.

It is possible for the chemical model to produce negative concentrations. However, the SIS, UGAMP and 4th order Runge Kutta methods conserve the total number of atoms and so any negative concentration will be compensated for by an 'overshoot' in one or more of the other species of the same chemical family. Using this property of conservation of the SIS scheme any negatives occurring after the chemical integration are corrected in the following way. For a chemical family (in this section the word 'family' is used to mean the sum of all odd chlorine species for example) of n members $(A_1, A_2, ... A_n)$ the following quantities are evaluated

$$P_A = \sum_{i=1}^n A_i \qquad (for A_i \ge 0)$$

$$N_A = \sum_{i=1}^{n} A_i \qquad (for A_i < 0)$$

Then the members of the family are corrected as follows:

$$A_i' = 0 (for A_i < 0)$$

$$A_i' = A_i \left(1 + \frac{N_A}{P_A} \right) \qquad (for A_i \ge 0)$$

Therefore the concentrations of the species in family A are adjusted whilst keeping the total family concentration constant. The negative mixing ratios are set to zero and this negative mass is partitioned around the other members of the family in proportion to their concentration. Note that this method corrects negatives within a model grid box; there is no borrowing from surrounding boxes.

A potential problem arises when a species is contained in more than one family. With the chemical scheme adopted the species concerned are $ClONO_2$, $BrONO_2$ and BrCl. As the abundance of Br_y species (pptv) is a lot smaller than the abundance of Cl_y and Br_y species (ppbv) $BrONO_2$ and BrCl are considered to the primarily in the Br_y family. If their concentrations are corrected due to negatives in the BrO_y family then the ClO_y and/or NO_y families are adjusted accordingly. Similarly, $ClONO_2$ is considered to be primarily in the ClO_y family.

Negative species concentrations can also be caused the model transport scheme. This is especially true for a spectral scheme as used in UGCM, for example. In general, a transport scheme will tend to produces negative tracer concentrations in regions of strong tracer gradients. By transporting species together in families the problem can be greatly ameliorated although not completely eliminated. In general, a transport scheme, even if it produces negative concentrations, will tend to conserve the global amount of a tracer. Therefore, although the above method for correcting negatives caused by the chemistry could also be used here, it may not be appropriate.

The method described here is a way of correcting for negative species concentrations. However, no correction will be ideal and a far better approach is to prevent the negatives from occurring in the first place by the use of a small enough timestep, a well formulated chemistry code and a decent transport scheme.

6 Heterogeneous Chemistry

A fairly detailed treatment of the heterogeneous chemical reactions which are believed to be important in the stratosphere is included in the model. This includes reactions occurring both on the surface of frozen polar stratospheric clouds (PSCs) and on liquid aerosols in the lower stratosphere sulphate layer. The model does not contain any microphysics and the particles are treated as being in equilibrium. A full microphysical calculation would be too expensive in terms of computer time and storage for the basic model.

The following heterogeneous reactions are treated in the model, although not all of these reactions occur on all of the different aerosols.

In order to prevent the addition of more species to the model the Cl_2 produced in reactions (152) and (154) is assumed to give 2 ClO_x molecules. The ClNO_2 produced in reaction (153) is assumed to give one ClO_x and one NO_x molecule. Br₂ and BrNO₂ are treated similarly.

The rate of the chemical reactions on an aerosol surface is generally parameterised as [see e.g. Rodriguez et al., 1989]:

$$\frac{-d[ClONO_2]}{dt} = k'_{152}[ClONO_2]$$

where k'_{152} is an equivalent first order rate constant for reaction (152), for example, which is calculated from:

$$k'_{152} = \frac{1}{4} \overline{\nu}_{ClONO2} \gamma_{152} \overline{A}$$

 \overline{A} is the available particle surface area and $\overline{\nu}_{ClONO2}$ is the mean speed of a ClONO₂ molecule which, from kinetic theory, is given by:

$$\overline{\nu}_{ClONO2} = \sqrt{\frac{8k_bT}{\pi.m_{ClONO2}}}$$

 k_b is Boltzmann's constant and m_{ClONO2} is the mass of a ClONO₂ molecule. The available surface area is calculated depending on the particles concerned. The reaction probabilities (γ) are taken from experimental data for each reaction and aerosol type. The values used are given in the table below. These are taken from NASA/JPL [1994] unless stated otherwise.

Reaction	Reaction	n Probal	oility (γ)	
	Liquid aerosol	SAT	NAT	Ice
150	0.1	0.006	0.0003	0.01
151	c	c	c	0.1
152	c	c	c	0.2
153			0.003	0.03
154	c		0.1	0.3
155	c		0.12	0.1
156	\mathbf{c}		0.25	0.3
157	\mathbf{c}		0.1	0.3
158			0.3	0.3
159			0.3	0.3
160			0.3	0.3
161	\mathbf{c}		0.006	0.3
162			0.005	0.005

Table 3. Reaction probabilities for heterogeneous reactions on liquid and solid aerosols. Notes: i) γ values in *italics* are assumed. ii) A 'c' means that the γ value is calculated (e.g. as a function of aerosol composition and/or temperature, see below).

6.1 Liquid Aerosols

The composition of liquid $H_2O/H_2SO_4/HNO_3/HCl$ aerosols is calculated using the analytical scheme of Carslaw et al., [1995a, 1995b] (in the subroutine LACOMP). This routine also calculates the solubilities of HBr, HOBr and HOCl. The total sulphate mixing ratio, required by the routine LACOMP, is specified and passed as an argument to the chemical model from e.g. the transport model. The model calculates the equilibrium vapour pressure of H_2SO_4 following an expression of Ayers et al., [1980]. This is the tested against the model H_2SO_4 field and used to switch off the liquid aerosol reactions in the upper stratosphere.

The rates of heterogeneous reactions on liquid aerosol are calculated in the subroutine HETLA. The rate of reactions (151) and (152) are parameterised following Hanson and Ravishankara [1994], using the HCl solubility of Luo et al. [1995]. The γ for reaction (161) on liquid aerosol is parameterised following the results of Hanson et al., [1996].

6.2 Sulphuric Acid Tetrahydrate

The heterogeneous rates on SAT particles are calculated in the subroutine HETSAT. The presence of SAT particles is tested by calculating the temperature of SAT point from:

$$T_{sat} = \frac{3236.0}{11.502 - \log(760pw)}$$

where pw is the partial pressure of H_2O in atmospheres. For reaction (152) the γ is calculated using the data of Hanson and Ravishankara [1993] and reaction (151) the γ is fitted as a function of the saturation ratio with respect to ice from the data of Zhang et al. [1994].

6.3 Nitric Acid Trihydrate

For NAT PSCs (HNO₃.3H₂O) the model mixing ratios of HNO₃ and H₂O and temperature are used with the expression of Hanson and Mauersberger [1988a] to predict when they are thermodynamically possible. The available surface area is calculated from the amount of HNO₃ condensed assuming that there are 10 NAT particles cm⁻³. The heterogeneous rates on NAT particles are calculated in the subroutine HETNAT.

Because NAT particles can be very large, gas diffusion limitation is taken into account. The first order loss rates are then calculated using

$$k'_{152} = \frac{\frac{1}{4}\overline{\nu}_{ClONO2}\gamma_{152}\overline{A}}{1 + \frac{3\gamma_{152}r_{nat}}{4l}}$$

from Turco et al. [1989], where l is the mean free path and r_{nat} is the radius of the NAT particle.

For reactions (151) and (152) the γ 's are calculated using the data of Hanson and Ravishankara [1993]. HCl and HBr are assumed not to dissolve into the NAT particles. Earlier work has given solubilities for HCl, e.g. Hanson and Mauersberger [1988b] but this is not used in the current model.

6.4 Ice Particles

The heterogeneous rates on ice particles are calculated in the subroutine HETICE. The existence of ice particles is tested using the following Teten's equation [Murray, 1967]:

$$p_s = 610.78 exp(21.875 \frac{T - 273.16}{T - 7.66})$$

where p_s is the saturation pressure (Pa) of H_2O over ice at temperature T(K). As for NAT, HCl and HBr are assumed not to dissolve in the ice particle. HNO₃ is removed from the gas phase in the presence of ice particles using the equilibrium NAT expression [Hanson and Mauersberger, 1988a]. This assumes a NAT coating (as opposed to a liquid coating) to the ice particles. The available surface area is calculated from an estimate of the amount of H_2O which is condensed and assuming that the radius of the ice particles formed is $10\mu m$.

NAT and ice particles can be sedimented from the model (switch LSED) with fall velocities appropriate for particles of radius 1μ m and 10μ m respectively.

7 Using The TOMCAT Chemical Scheme

The standard chemical model described here is available on the RAL Cray in the nupdate library /home/j90/kd/tomcat/TOMCATI. Example jobdecks for TOMCAT and SLIMCAT are given in /home/j90/kd/tomcat/jobs and /home/j90/kd/slimcat/jobs. The model is also available on the Cambridge Suns in the directory /home/martyn/TOMCAT/BOXMODI. The basic code is contained in the two files boxmod.f and photolib.f. Makefile.c can be used to compile and run the program. On the suns the separate nupdate common decks (e.g. PARCHI) are saved as separate files with the same name.

7.1 Common Decks

The common decks used by the model are listed here:

Name	Description	
CONCS	Concentration of chemical species	
COND	Concentration of condensed species	
CROSSEC	Absorption cross sections	
DISSOC	Photolysis rates	
DO3DT	Rates in the O_3 budget	
EQUILM	Indicator of photochemical equilibrium (OClO, BrCl, NO ₃)	
IIGAS	Index of chemical species for CONC array	
PARCHI	Parameters for chemistry	
PARPHO	Parameters for photolysis routines	
RATEK	Thermal rate constants	
RATIOS	Ratios of species within families	
SWITCH	Switches to control model	
TABJS	Definition of photolysis look up tables	

7.2 Subroutines

The principal subroutines of the model are listed here:

Name	Description
CALCJS	Looks up the photodissociation coefficients
CALCKS	Calculates the thermal rate constants
CHIMIE	Interface between the chemical model and the transport/trajectory model
COLMOD	Main subroutine of the chemical model
CORNEG	Corrects negative concentrations
CRATIO	Partitions species within chemical families
DERIVS	Calculates rates for ODEIMP and ODEINT
DOZNEDT	Diagnoses terms in O_3 budget
INIJTAB	Initialises photolysis look-up tables
INISIS	Integrates long-lived species
JACOBI	Calculates Jacobian diagonal for ODEIMP
HETICE	Calculates heterogeneous rates on ICE particles
HETKEM	Principal subroutine for heterogeneous chemistry
HETLA	Calculates heterogeneous rates on liquid aerosols
HETNAT	Calculates heterogeneous rates on NAT particles
HETSAT	Calculates heterogeneous rates on SAT particles
LACOMP	Calculates liquid aerosol composition
MATRIX	Inverts the matrix \mathbf{M} for SIS scheme
ODEIMP	Integrates chemistry using UGAMP method
ODEINT	Integrates chemistry using Runge Kutta method
OUTVMR	Outputs mixing ratios for paper listing
SISINT	Creates the matrix \mathbf{M} for SIS scheme

7.3 Fortran Channels

The model makes use of the following fortran channels during execution:

Channel	Variable	Common Deck	Purpose
71	NOUT	PARCHI	Output of species in OUTVMR
72	NSTD	PARPHO	Reading standard atmosphere profiles
80	NTAB	PARPHO	Reading/writing photolysis table jtable

7.4 Photolysis Tables

When the model is run the subroutine INIJTAB writes out the photolysis look up tables to the file jtable. As the creation of the look-up tables is expensive, this file can be saved for use in subsequent runs (so long as the same parameters in PARPHO are still used). In this case the call to INIJTAB should be commented out. The subroutine CALCJS obtains the photolysis rates by linear interpolation on the tabulated J rates in zenith angle, log(pressure), temperature and ozone column. Obviously, photolysis rates do not necessarily depend on these quantities in a linear way but linear interpolation is inexpensive and does not produce undershoots or overshoots. The photolysis table should therefore be set up with enough coordinates in the four dimensions to reduce errors due to the linear interpolation.

The parameters for the photolysis routines are set up in the common deck PARPHO:

Parameter	Meaning
NIN	Number of altitudes in STDT03 file
JPLEV	Number of pressure altitudes in jtable
JPCHI	Number of solar zenith angles in jtable
SZAMAX	Maximum solar zenith in jtable
JPS90	Number of solar zenith angles $> 90^{\circ}$ in jtable
JPTEM	Number of temperature values in jtable
TMIN	Minimum temperature in jtable (K)
TMAX	Maximum temperature in jtable (K)
JP03P	Number of O ₃ column factors in jtable
O3MIN	Minimum O_3 column factor $(0 < O3MIN < 1)$
CAMAX	Maximum O_3 column factor $(1 < O3MIN)$

7.5 Chemical Integration Scheme

The choice of integration scheme for the short-lived species is controlled by the variable IINT in the common deck SWITCH.

IINT	Scheme	Comment
1	SIS	Default and recommended scheme
2	UGAMP	
3	NCAR	
4	Runge Kutta	Expensive

7.6 Heterogeneous Chemistry

The choice of heterogeneous chemistry scheme is controlled by the variable IHET in the common deck SWITCH.

IHET	Scheme	Comment
0	None	only gas phase chemistry
1	LA/NAT/ice	
2	LA/ice	
3	LA/SAT/NAT/ice	
4	NAT/ice	
5	SAT only	
6	NAT only	
7	LA only	

Sedimentation of NAT and ice particles can be switched on by setting the switch LSED in HETKEM to TRUE.

7.7 Inlined Subroutines

To speed up the model on the Cray certain short subroutines are 'inlined' during compilation. These subroutines are EI1, EI2, EI3, THREEB and RKBACK. The file mpc/BIBLI/inlini.f contains the copies of these subroutine which are inlined.

7.8 Interface With Chemical Scheme

The principal subroutine of the chemical scheme is COLMOD. The arguments passed to this subroutine are:

SUBROUTINE COLMOD(F, IHMIN, IHMAX, DTIME, CONCM, PPA, PLA,

- + T,Z03,ZN,ZN0,ZN02,ZN03,ZN205,ZH20,ZHN03,
- + ZCLNO3, ZCLO, ZHCL, ZHNO4, ZHOCL, ZCL, ZO,
- + ZCL202, ZOCLO, ZBR, ZBRO, ZBRNO3, ZBRCL, ZH202,

```
+ ZOX,ZNOX,ZCLX,ZBRX,ZHOBR,ZHBR,
+ ZN20,ZC0,ZCH4,Z01D,ZH,Z0H,ZHO2,
+ ZCH3CL,ZF22,ZF113,ZMCFM,ZCCL4,
+ ZF12B1,ZF13B1,ZCH3BR,ZHF,ZCOF2,ZCH20,ZCOFCL,
+ ZF11,ZF12,ZH2SO4,ZCH3,ZHC0,ZCH302,ZMHP,ZCH30,
+ ZH2OS,ZHNO3S,ZHBRS,ZHCLS,
+ TROP,O3COL,IUBOX,IDDT,ICJS,RLAT,ICKS)
```

Variable	Dimension	Description
F	LNT	Cosine(solar zenith angle)
IHMIN	1	Minimum index for loops
IHMAX	1	Maximum index for loops
DTIME	1	Chemical timestep (s)
CONCM	LNT	[M] (molecules cm ⁻³)
PPA	LNT	Pressure at box centre (Pa)
PLA	LNT,0:1	Pressure at top (0) and bottom (1) of box (Pa)
T	LNT	Temperature (K)
Z03	LNT	Volume mixing ratio of O ₃
ZH2SO4	LNT	Total sulphate volume mixing ratio
TROP	LNT	Flag for troposphere (=0 for strat. =1 for trop)
O3COL	LNT	Column O_3 above box (molecules cm ⁻²)
IUBOX	LNT	Index of box above current box
IDDT	1	Number of chemical subtimestep
ICJS	1	Controls calculation of J rates
RLAT	1	Latitude (degrees). Used in PSC test.
ICKS	1	Controls calculation of rate constants

8 Tests

8.1 Compiler Tests

On a Sun workstation the following compilation tests were performed:

- The model compiles with no ERRORS or WARNINGS.
- The model subroutines use IMPLICIT NONE statements to guard against undefined variables.
- The model was checked for arrays going out of bounds (-C in f77) with no errors.

On the Cray J90 the following compilation tests were performed: $\,$

- The model compiles with no ERRORS or WARNINGS.
- The model runs with variables initialised indefinite (-f indef).
- The model was checked for arrays going out of bounds (-Rbc in cft77).

8.2 Box Model Tests

The stability and accuracy of the model's integration schemes, and its treatment of families, were tested in a number of box model integrations. The model was integrated along 4 different idealised 'trajectories' corresponding to different photochemical regimes: a) polar lower stratosphere, b) mid stratosphere, c) upper stratosphere and d) mesosphere. The trajectories were all 100 days long. Apart from trajectory A, the initial chemical conditions used were not necessarily realistic but that is not important here for these tests of numerical stability and accuracy.

Trajectory	P/hPa	SIS	Runge Kutta	UGAMP	SIS
		(family)			(no families)
A polar	50	A1	A2	A3	A4
В	5	B1	B2	В3	B4
C	2	C1	C2	C3	C4
D	0.2	D1	D2	D3	D4

Table 4. Trajectory test experiments.

8.2.1 Integration Scheme

Figures 1 to 4 show results for 3 different integration schemes in the basic chemical model with families. In all cases the 4th order Runge Kutta scheme can be taken as a benchmark. The default SIS scheme and the UGAMP scheme (with 20 Newton Raphson iterations) all behave well. For polar trajectory A, the SIS scheme does give very slightly less O_3 destruction.

8.2.2 Use of Families

Figures 1 to 4 also show a comparison of the model integrated without families and with no assumption of photochemical equilibrium. In this version of the model (boxnof.f) all species are integrated separately. This tests the formulation of families within the basic model. The comparisons are very similar. The most critical area for this comparison is in the lower stratosphere where rate determining steps in catalytic cycles appear in the ratio expressions. The model without families does give slightly more O₃ loss for trajectory A, but the performance of the basic model is satisfactory.

8.3 Photolysis Rates

Figure 5 shows profiles of selected photolysis rates from the model for a solar zenith angles (SZA) of 37° with a surface albedo of 0.35. The photolysis rates appear reasonable (e.g. compare with plot in NASA/JPL [1994]) and this figure is included as a guide to typical model photolysis rates.

8.4 Heterogeneous Chemistry

The chemical model was integrated along an idealised trajectory in the polar lower stratosphere to test the heterogeneous chemistry schemes. Eight experiments were performed with the parameter IHET set from 0 to 7. The results for HCl and ClONO₂ are shown in Figure 6. It is not appropriate to discuss the details of these experiments in this report, but the figure shows that the various schemes do activate chlorine efficiently in polar winter conditions.

8.5 Coupling to 2D Transport Model

In the near future 3D chemical models will probably replace 2D models as the main tool for long term stratospheric assessment studies. As well as the dynamical problems associated with 2D models, the chemical schemes used in these models often employ diurnal averaging and use large chemical families. To test the stability of the TOMCAT chemical scheme for long integrations I coupled the model to the 2D model developed by Kinnersley [1996].

Figure 7 shows selected fields from the TOMCAT chemistry scheme (without heterogeneous chemistry) coupled to the 2D model after 940 days of integration. Also shown are the equivalent fields from the 2D model with the original 2D model chemistry scheme. The comparison is good and shows that the TOMCAT scheme is stable for long integrations. Minor differences are expected because of the different photolysis treatments, different families, day averaging in the 2D model scheme etc.

Figure 8 shows a comparison of column O3 from the TOMCAT chemical scheme (without heterogeneous chemistry) coupled to the 2D model (towards the end of a 1000 day integration) along with the same plot from

the original 2D model code. The TOMCAT scheme has larger O_3 columns by around 20 DU in the tropics and by up to 70 DU in the northern hemisphere spring. The large O_3 columns in this region are unrealistic. This is worth noting but the subtle balance of O_3 chemistry and dynamics in the lower stratosphere is difficult to capture in a 2D model and so it is not possible to ascribe the large O_3 columns to deficiencies in the TOMCAT chemistry scheme.

8.6 Domain Filling Trajectories

As the TOMCAT chemical scheme described here is designed to be efficient in a 3D model, it is very suitable for integrating chemistry along a large number of domain filling trajectories. The structure of the code does not require gridboxes to be adjacent.

8.7 3D Transport Model

The main purpose of the chemical model described here is to be coupled with a 3D chemical transport model (e.g. TOMCAT or SLIMCAT). Numerous experiments have been performed with earlier versions of the chemical code described here.

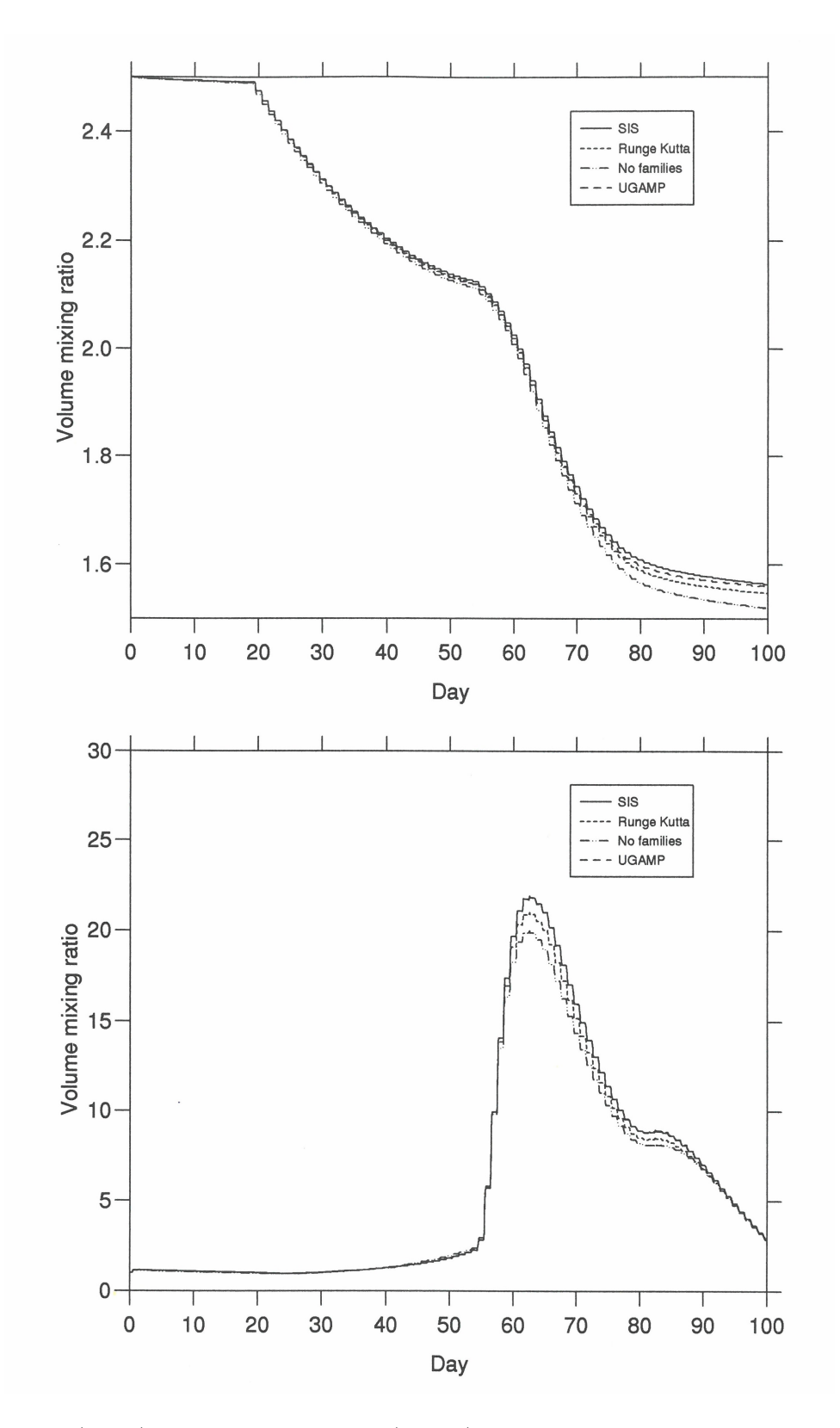


Figure 1: Above: O_3 (ppmv) from polar trajectory A (50 hPa) for 4 different box model runs. The model without chemical families, and without assumption of photochemical equilibrium for the HO_x and CHO_x species, shows sightly larger ozone depletion. Among the 3 different integration schemes in the model with chemical families, the default SIS scheme gives very slightly less ozone depletion. Below: H_2O_2 (pptv) from trajectory A. In this plot SIS and UGAMP curves are identical.

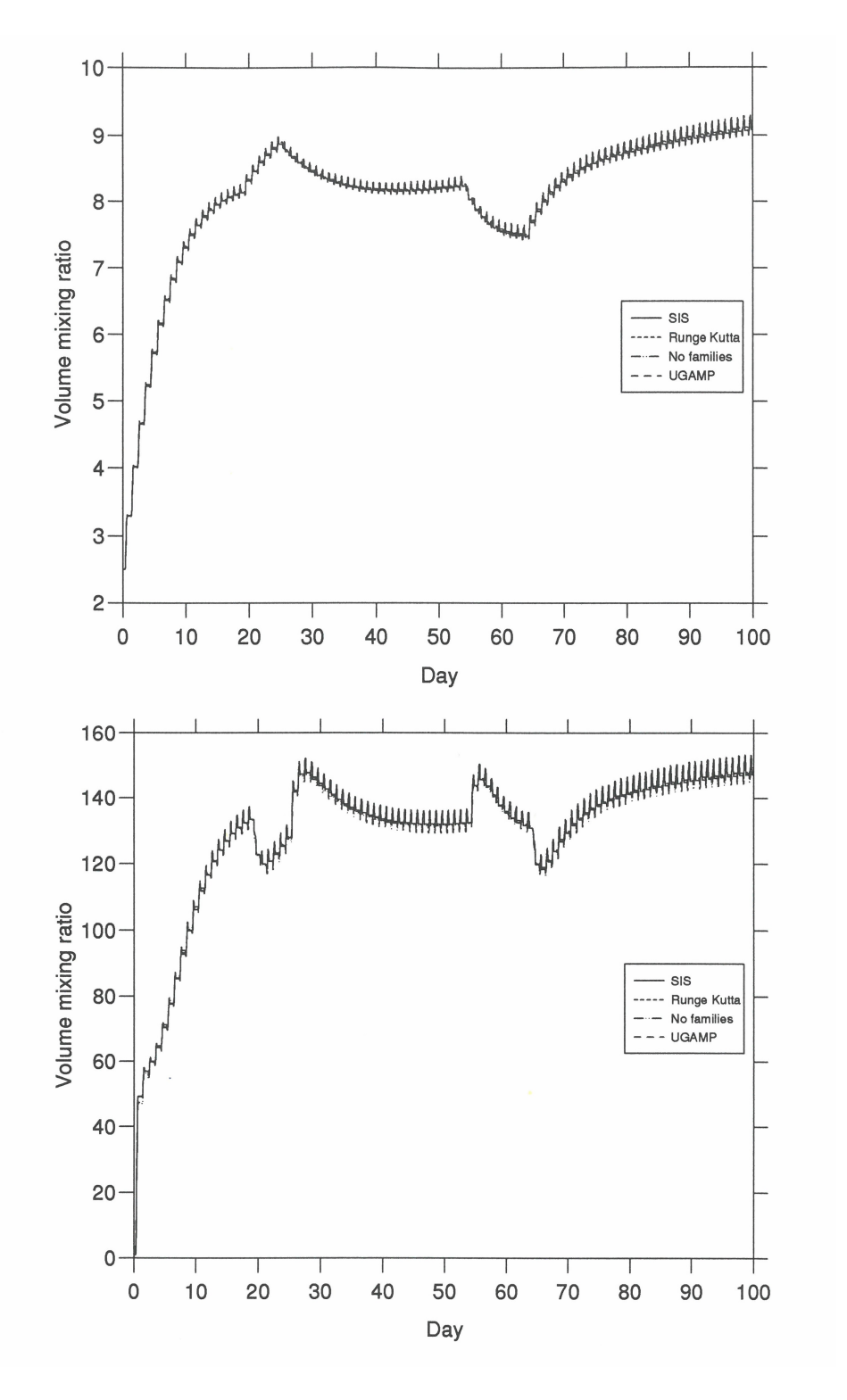


Figure 2: Above: O_3 (ppmv) from trajectory B (5 hPa) for 4 different box model runs. At this altitude the model without families and the 3 different integration schemes in the model with families all give virtually identical results. Below: H_2O_2 (pptv) from trajectory B.

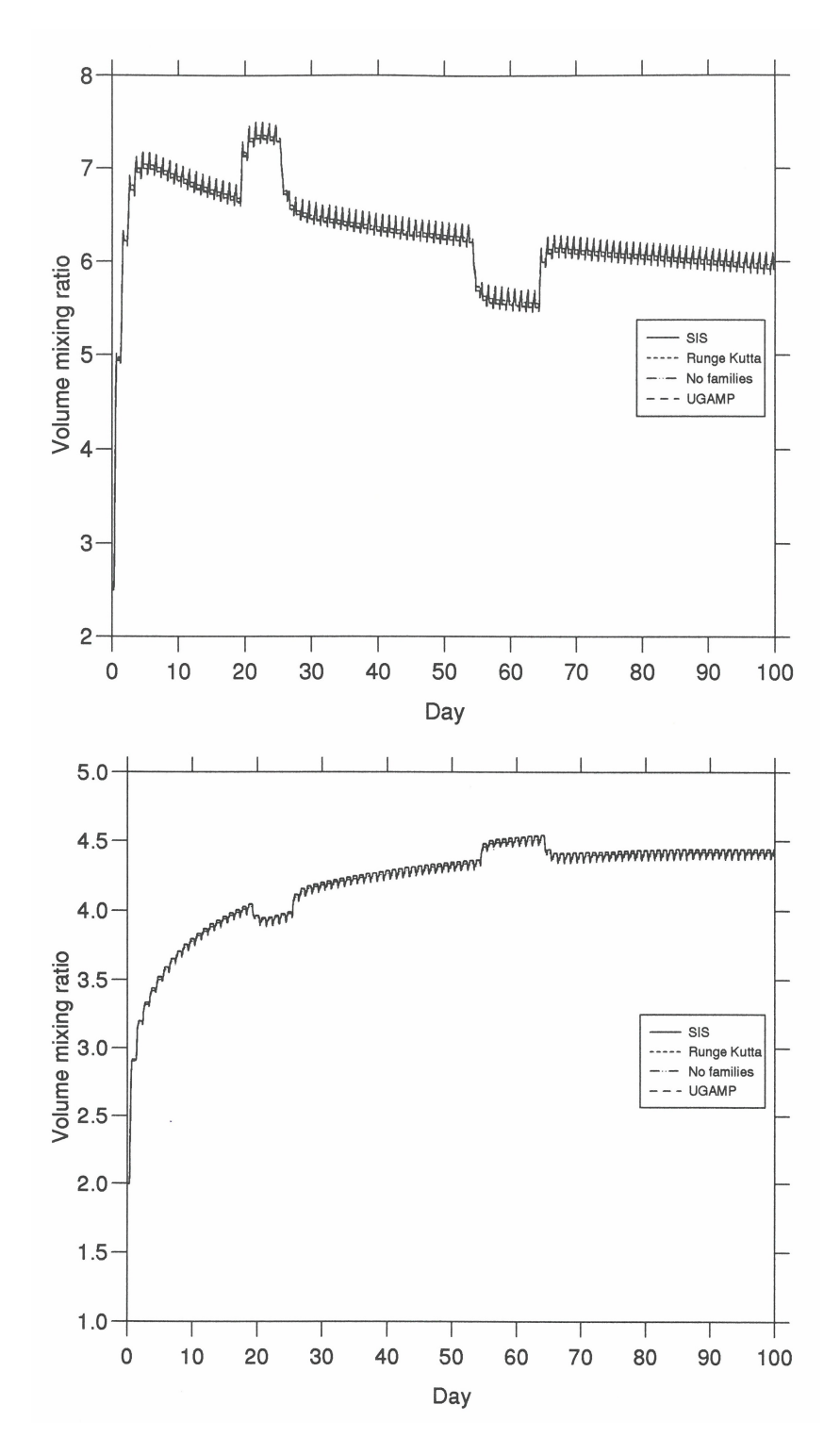


Figure 3: Above: O_3 (ppmv) from trajectory C (2 hPa) for 4 different box model runs. At this altitude the model without families and the 3 different integration schemes in the model with families all give virtually identical results. Below: HCl (ppbv) from trajectory C.

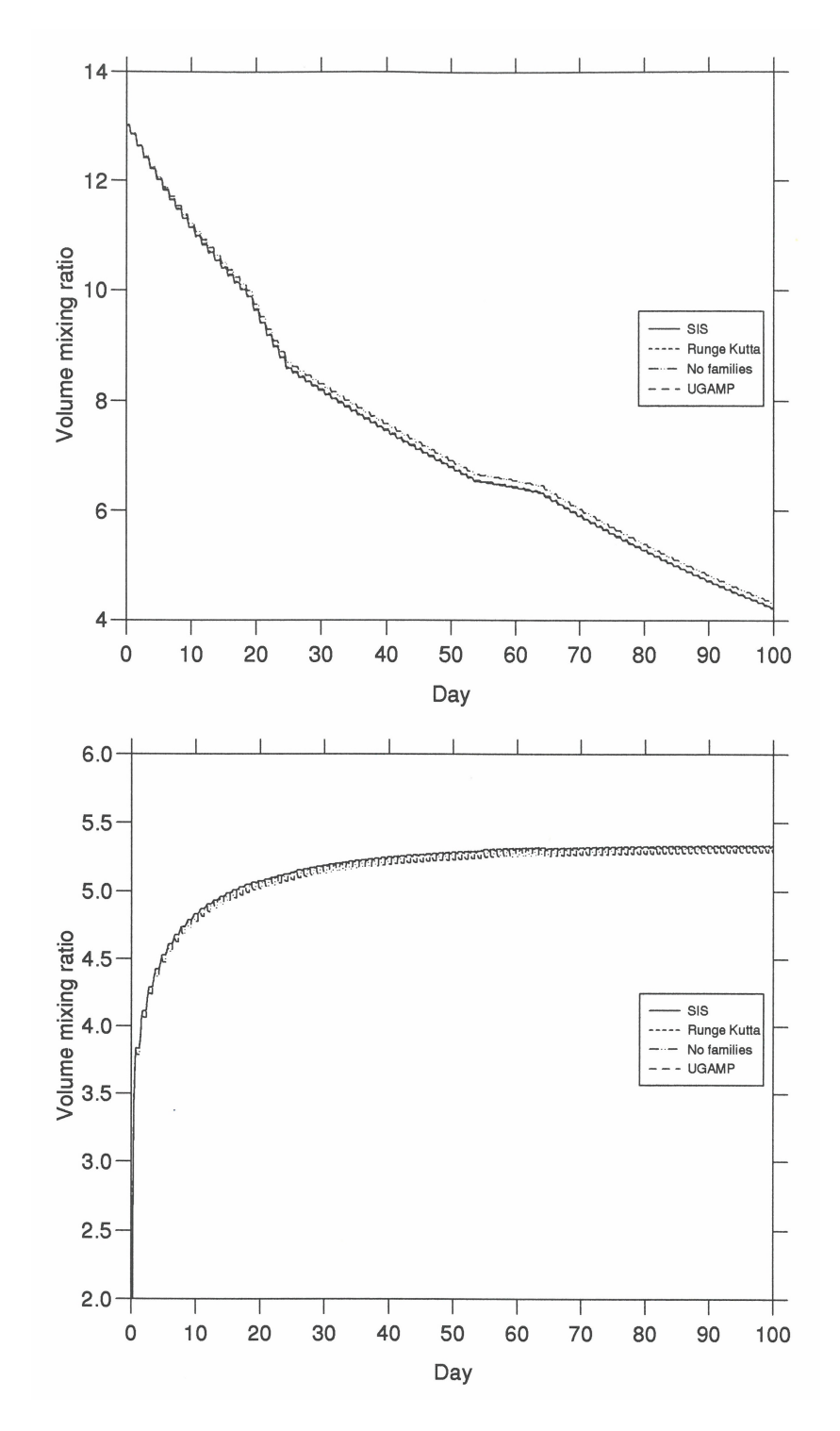


Figure 4: Above: NO_y (ppbv) from trajectory D (0.2 hPa) for 4 different box model runs. The model without families gives slightly less NO_y destruction. Below: HCl (ppbv) from trajectory D.

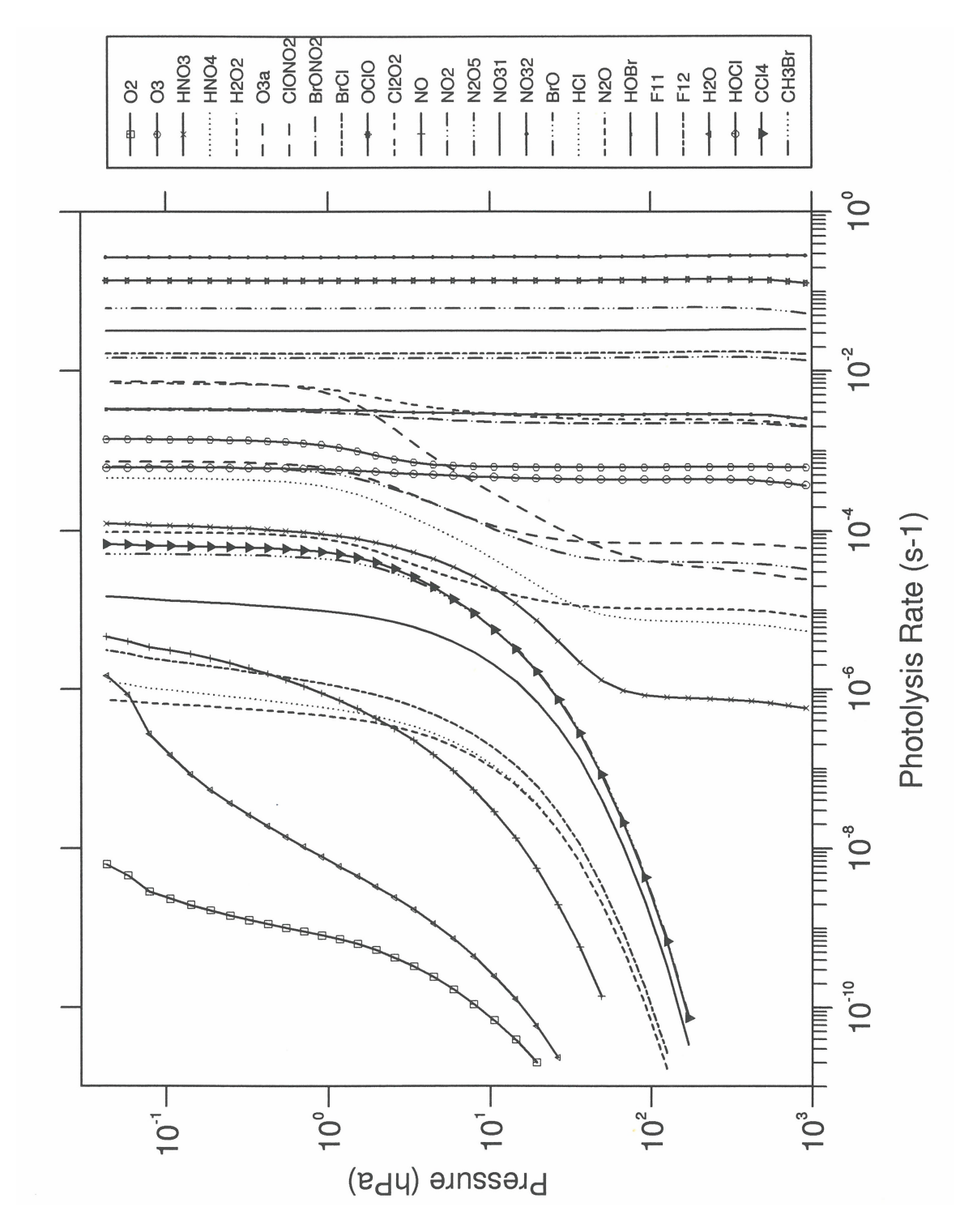


Figure 5: Profiles of selected photolysis rates from the TOMCAT chemical scheme. SZA= 37^{o} , albedo=0.35.

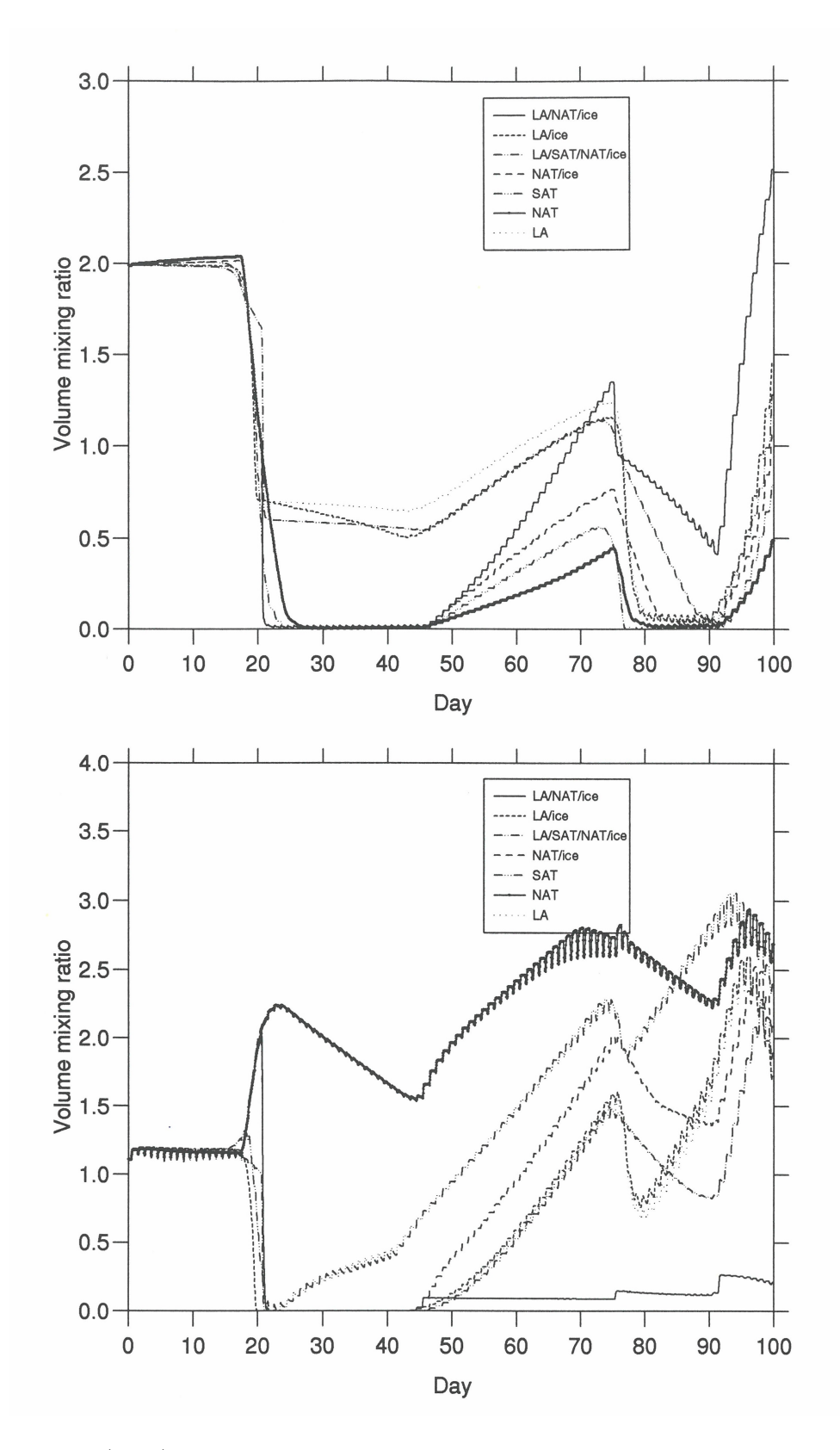


Figure 6: Above: HCl (ppbv) for different heterogeneous schemes on an idealised trajectory at 50 hPa with 2 'PSC' events near days 20-40 and days 80-90. Below: $ClONO_2$ (ppbv) for the same experiments.

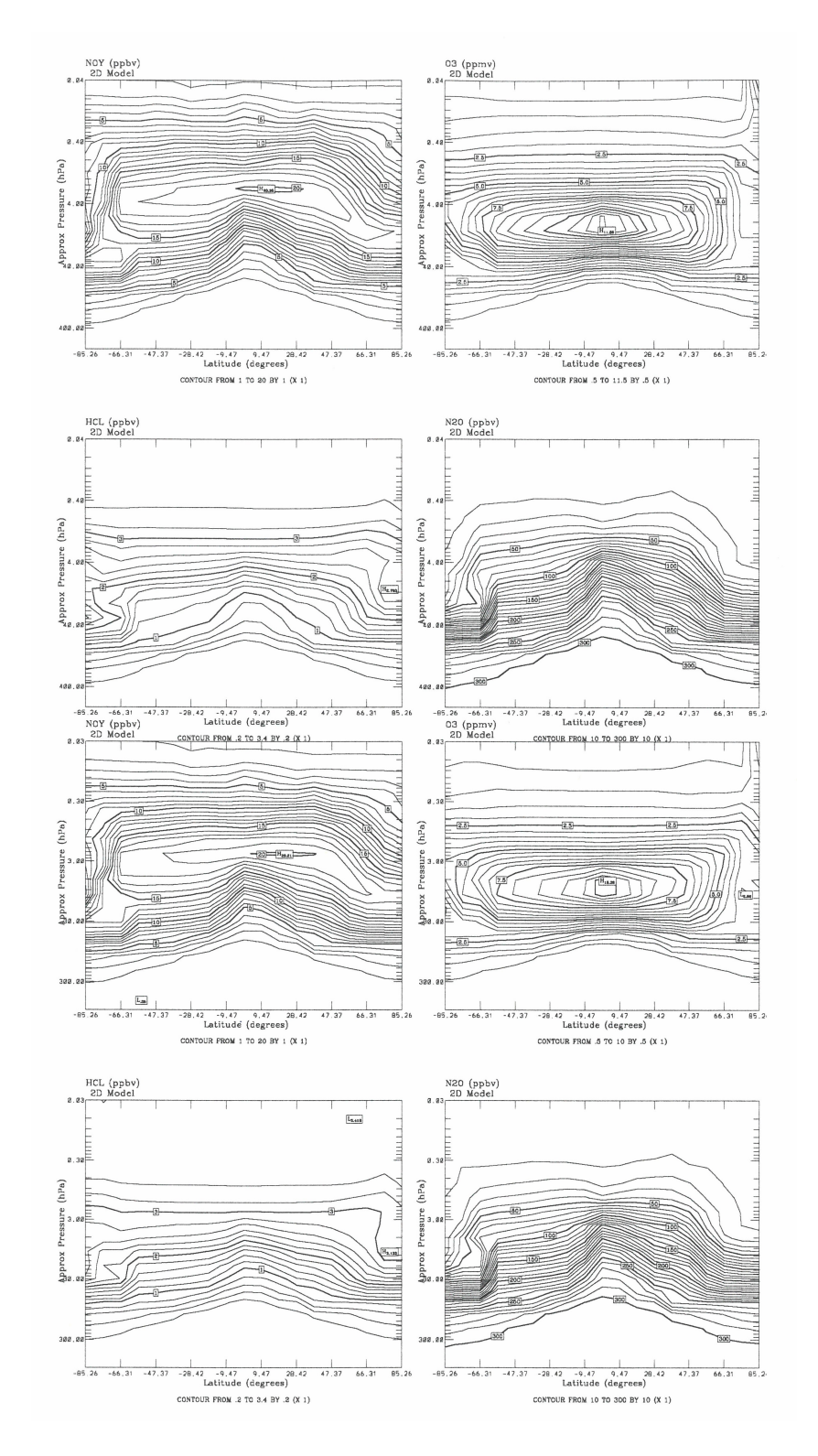


Figure 7: Above: Latitude-height plots of NO_y , O_3 , N_2O and HCl from the TOMCAT chemistry scheme coupled with a 2D latitude-height model for October after 940 days of integration. Below: Similar plot from the 2D model with standard 2D model chemical scheme.

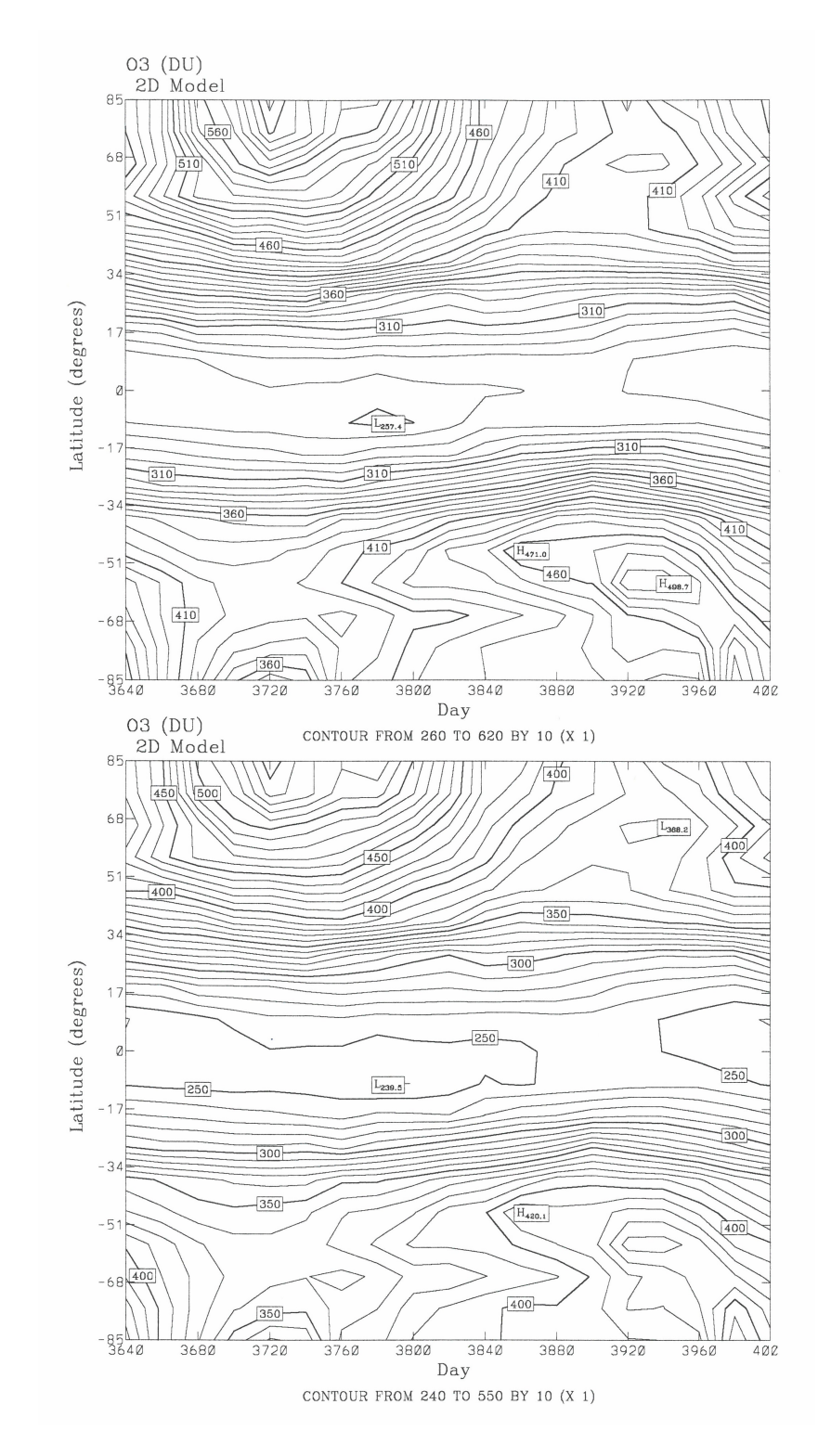


Figure 8: Above: Latitude-time plot of column O_3 from the TOMCAT chemistry scheme coupled with a 2D latitude-height model. Below: Similar plot from the 2D model with standard 2D model chemical scheme. Time axes run from January to December.

9 Summary

This report has described the TOMCAT stratospheric chemistry model designed to be coupled to a 3D transport model. The model can be used for a variety of applications but it is intended to be particularly efficient for use in 3D atmospheric model on a vector supercomputer. The efficiency of the code on a Cray is illustrated by the flowtrace from the model shown in Appendix 4.

10 Acknowledgements

This chemical model has benefited from several collaborations at various stages. I am grateful to the following people for their help: Richard Ramaroson (SIS integration scheme), Glenn Carver and Peter Stott (UGAMP integration scheme), David Lary (photolysis scheme), Ken Carslaw and Thomas Peter (heterogeneous chemistry).

References

- [1] Allen, M., and J.E. Frederick, Effective photodissociation cross sections for molecular oxygen and nitric oxide in the Schumann-Runge bands, *J. Atmos. Sci.*, 39, 2066-2075, 1982.
- [2] Ayers, G.P., R.W. Gillett, and J.L. Gras, On the vapor pressure of sulfuric acid, *Geophys. Res. Letts.*, 7, 433-436, 1980.
- [3] Brasseur, G., and S. Solomon, Aeronomy of the Middle Atmosphere, 1984.
- [4] Carslaw, K., B. Luo, and T. Peter, An analytic expression for the composition of aqueous HNO₃-H₂SO₄ stratospheric aerosols including gas phase removal of HNO₃, *Geophys. Res. Lett.*, 22, 1877-1880, 1995a.
- [5] Carslaw, K.S., S.L. Clegg, and P. Brimblecome, A thermodynamic model of the system HCl-HNO₃-H₂SO₄-H₂O, including solubilities of HBr, from < 200 K to 328 K, J. Phys. Chem., 99, 11557-11574, 1995b.</p>
- [6] Chipperfield, M.P., and P. Simon, The TOMCAT offline chemical transport model. Part II. Dynamics and Advection, UGAMP Internal Report No. 44b. 1996.
- [7] Dongerra, J.J., et al., LINPACK User's Guide, Philadelphia: Society for Industrial and Applied Mathematics, 1979.
- [8] Hanson, D., and K. Mauersberger, Laboratory studies of the nitric acid trihydrate: implications for the south polar stratosphere, *Geophys. Res. Lett.*, 15, 855-858, 1988a.
- [9] Hanson, D., and K. Mauersberger, Solubility and equilibrium vapor pressures of HCl dissolved in polar stratospheric cloud material: Ice and the trihydrate of nitric acid, *Geophys. Res. Lett.*, 15, 1507-1510, 1988b.
- [10] Hanson, D.R., and A.R. Ravishankara, Reaction of $ClONO_2$ with HCl on NAT, NAD and frozen sulfuric acid and hydrolysis of N_2O_5 and $ClONO_2$ on frozen sulfuric acid, J. Geophys. Res., 98, 22931-22936, 1994.
- [11] Hanson, D.R., and A.R. Ravishankara, Reactive uptake of ClONO₂ onto sulfuric acid due to reaction with HCl and H₂O, *J. Phys. Chem.*, 98, 5728-5735, 1994.
- [12] Hanson, D.R., A.R. Ravishankara, and E.R. Lovejoy, Reaction of BrONO₂ with H₂O on submicron sulfuric acid aerosol and the implications for the lower stratosphere, *J. Geophys. Res.*, 101, 9063-9069, 1996.
- [13] Hanson, D.R., A.R. Ravishankara and S. Solomon, Heterogeneous reactions in sulfuric acid aerosols: A framework for model calculations, *J. Geophys. Res.*, 99, 3615-3629, 1994.
- [14] Kinnersley, J.S., The climatology of the stratospheric THIN AIR model, Q. J. R. Meteorol. Soc, 122, 219-252, 1996.

- [15] Lary, D.J., Photochemical studies with a three-dimensional model of the atmosphere, PhD Thesis, Cambridge University, 1991.
- [16] Lary, D.J., and J.A. Pyle, Diffuse radiation, twilight and photochemistry, J. Atmos. Chem., 13, 373-392, 1991.
- [17] Luo, B., et al., Vapour pressures of H₂SO₄/HNO₃/HCl/HBr/H₂O solutions to low stratospheric temperatures, *Geophys. Res. Lett.*, 22, 247-250, 1995.
- [18] Maric, D., J.P. Burrows, and G.K. Moortgat, A study of the UV-visible absorption spectra of Br₂ and BrCl, J. Photochem. Photobiol. A: Chem., 83, 179-192, 1994.
- [19] Meier, R.R., D.E. Anderson, and M. Nicolet, Radiation field in the troposphere and stratosphere from 240-1000 nm. I. General analysis. *Planet. Space Sci.*, 30, 923-933, 1982.
- [20] Michelsen, H.A., R.J. Salawitch, P.O. Wennberg and J.G. Anderson, Production of O(¹D) from photolysis of O₃, Geophys. Res. Lett., 21, 2227-2230, 1994.
- [21] Murray, F.W., On the computation of saturation vapour pressure, J. Appl. Met., 6, 203-204, 1967.
- [22] NASA/JPL, W.B. DeMore et al, Chemical kinetics and photochemical data for use in stratospheric modelling, Evaluation no. 11, JPL publication 94-1, 1994.
- [23] Nicolet, M., R.R. Meier, and D.E. Anderson, Radiation field in the troposphere and stratosphere from 240-1000 nm. I. Numerical analysis. *Planet. Space Sci.*, 30, 935-983, 1982.
- [24] Numerical Recipes, The Art of Scientific Computing (Fortran Version), by W.H. Press, B.P. Flannery, S.A. Teukolsky and W.T. Vetterling, Cambridge University Press, 1990.
- [25] Prather, M.J., Numerical advection by conservation of second order moments, J. Geophys. Res., 91, 6671-6681, 1986.
- [26] Ramaroson, R.A., Modelisation locale, à une et trois dimensions des processus photochimiques de l'atmosphère moyenne, PhD Thesis, Université Paris VI, 1989.
- [27] Ramaroson, R., M. Pirre and D. Cariolle, A box model for on-line computations of diurnal variations in a 1D model: Potential for application to multidimensional cases, *Ann. Geophysicae.*, 10, 416-428, 1992.
- [28] Rodriguez, J.M. et al, Nitrogen and chlorine species in the spring Antarctic stratosphere: comparison of models with airborne Antarctic ozone experiment observations, J. Geophys. Res., 94, 16,683-16,703, 1989.
- [29] D.Z. Stockwell and M.P. Chipperfield, The TOMCAT offline chemical transport model. Part III. Convection and vertical diffusion, UGAMP Internal Report No. 44c, 1996.
- [30] Stott, P.A., and R.S. Harwood, An implicit time-stepping scheme for chemical species in a global atmospheric general circulation model, *Ann. Geophysicae.*, 11, 377-388, 1993.
- [31] Turco, R.P., O.B. Toon, and P. Hamill, Heterogeneous physicochemistry of the polar ozone hole, *J. Geophys. Res.*, 94, 16493-16510, 1989.
- [32] Wahner, A., G.S. Tyndall, and A.R. Ravishankara, Absorption cross sections for OClO as a function of temperature in the wavelength range 240-480nm, *J. Phys. Chem.*, 91, 2734-2738, 1987.
- [33] Zhang, R., J.T. Jayne, and M.J. Molina, Heterogeneous interactions of ClONO₂ and HCl with sulfuric acid tetrahydrate: implications for the stratosphere, *J. Phys. Chem.*, 98, 867-874, 1994.

11 Appendix 1. Photochemical Reactions.

The photochemical reactions contained in the model are listed here.

1	O + O + M	$\rightarrow O_2 + M$
2	$O + O_2 + M$	$\rightarrow O_3 + M$
3	$O + O_3$	$\rightarrow 2O_2$
6a	$O(^{1}D) + N_{2}$	$\rightarrow O + N_2$
6b	$O(^{1}D) + O_{2}$	$\rightarrow O + O_2$
7	$O(^1D) + H_2O$	$\rightarrow 2OH$
8	OH + O	$\rightarrow H + O_2$
9	$O_2 + H + M$	$\rightarrow HO_2 + M$
10	$HO_2 + O$	$\rightarrow OH + O_2$
11	$OH + O_3$	$\rightarrow HO_2 + O_2$
12	$H + O_3$	$\rightarrow OH + O_2$
13	$OH + HO_2$	$\rightarrow H_2O + O_2$
14	OH + OH	$\rightarrow H_2O + O$
15a	$H + HO_2$	$\rightarrow OH + OH$
15b	$H + HO_2$	$\rightarrow H_2 + O_2$
15c	$H + HO_2$	$\rightarrow H_2O + O$
16	$NO_2 + O$	$\rightarrow NO + O_2$
17	$NO + O_3$	$\rightarrow NO_2 + O_2$
18	$NO_2 + O_3$	$\rightarrow O_2 + NO_3$
20	$HNO_3 + OH$	$\rightarrow H_2O + NO_3$
21	$NO_2 + OH + M$	$\rightarrow HNO_3 + M$
22	$O(^{1}D) + N_{2}O$	$\rightarrow 2NO$
22b	$O(^{1}D) + N_{2}O$	$\rightarrow N_2 + O_2$
24	$HO_2 + HO_2$	$\rightarrow H_2O_2 + O_2$
26	$H_2O_2 + OH$	$\rightarrow H_2O + HO_2$
29	$H_2O_2 + rain$	\rightarrow
30	$OH + CH_4$	$\rightarrow H_2O + CH_3$
31	$O(^1D) + CH_4$	$\rightarrow CH_3 + OH$
32	$O(^1D) + H_2$	$\rightarrow H + OH$
34	CO + OH	$\rightarrow CO_2 + H$
35	$NO + HO_2$	$\rightarrow NO_2 + OH$
36	$HO_2 + O_3$	$\rightarrow OH + 2O_2$
37	$HO_2 + NO_2 + M$	$\rightarrow HO_2NO_2 + M$
38	$HNO_3 + rain$	\rightarrow
39	$HO_2NO_2 + M$	$\rightarrow HO_2 + NO_2 + M$
40	$HO_2NO_2 + OH$	$\to H_2O + O_2 + NO_2$
41	$HO_2NO_2 + rain$	\rightarrow
48	$O(^{1}D) + CFCl_{3}$	$\rightarrow 2Cl + COFCl$
49	$O(^1D) + CF_2Cl_2$	$\rightarrow 2Cl + COF_2$

```
50
               Cl + O_3
                                     \rightarrow ClO + O_2
 51
               ClO + O
                                     \rightarrow Cl + O_2
 52
              Cl + H_2O_2
                                     \rightarrow HCl + HO_2
                                     \rightarrow Cl + NO_2
 55
              ClO + NO
 57
              Cl + CH_4
                                     \rightarrow HCl + CH_3
 58
               Cl + H_2
                                     \rightarrow HCl + H
 59
              Cl + HO_2
                                     \rightarrow HCl + O_2
59b
              Cl + HO_2
                                     \rightarrow OH + ClO
 60
              OH + HCl
                                     \rightarrow H_2O + Cl
 61
             HCl + rain
                                     \rightarrow
 62
          ClO + NO_2 + M
                                     \rightarrow ClONO_2 + M
 63
            ClONO_2 + O
                                     \rightarrow ClO + NO_3
             Cl + HOCl
                                     \rightarrow HCl + ClO
64b
 65
             HO_2 + ClO
                                     \rightarrow HOCl + O_2
65b
             HO_2 + ClO
                                     \rightarrow HCl + O_3
             OH + HOCl
                                     \rightarrow H_2O + ClO
 66
                                     \rightarrow OH + ClO
 67
              O + HOCl
 68
          ClO + ClO + M
                                     \rightarrow Cl_2O_2 + M
68b
             ClO + ClO
                                     \rightarrow 2Cl + O_2
68c
             ClO + ClO
                                     \rightarrow Cl + OClO
 69
             Cl_2O_2 + M
                                     \rightarrow ClO + ClO + M
               N + NO
 70
                                     \rightarrow N_2 + O
                                     \to NO + O
 71
               N + O_2
 72
                N + O_3
                                     \rightarrow NO + O_2
              OH + ClO
                                     \rightarrow Cl + HO_2
75a
              OH + ClO
                                     \rightarrow HCl + O_2
75b
            O(^1D) + CCl_4
 80
                                     \rightarrow 4Cl + products
          O(^{1}D) + CH_{3}Cl_{3}
                                     \rightarrow 3Cl + products
 81
           OH + CH_3Cl_3
                                     \rightarrow 3Cl + products
 82
 83
          O(^{1}D) + CH_{3}Cl
                                     \rightarrow Cl + products
 84
            OH + CH_3Cl
                                     \rightarrow Cl + products
         O(^{1}D) + CF_{2}ClH
 85
                                     \rightarrow Cl + COF_2 + products
           OH + CF_2ClH
                                     \rightarrow Cl + COF_2 + products
 86
         O(^1D) + C_2F_3Cl_3
 87
                                     \rightarrow 2Cl + COF_2 + COFCl + products
          NO_2 + NO_3 + M
                                     \rightarrow N_2O_5 + M
 91
 92
              N_2O_5 + M
                                     \rightarrow NO_3 + NO_2 + M
100
           CH_3 + O_2 + M
                                     \rightarrow CH_3O_2 + M
                                     \rightarrow CH_3O + NO_2
101
            CH_3O_2 + NO
           CH_3O_2 + HO_2
                                     \rightarrow CH_3OOH + O_2
102
         CH_3O_2 + CH_3O_2
                                     \rightarrow 2CH_3O + O_2
103
          CH_3OOH + OH
                                     \rightarrow CH_3O_2 + H_2O
104
                                     \rightarrow CH_2O + HO_2
105
             CH_3O + O_2
```

```
106
             CH_2O + OH
                                    \rightarrow CHO + H_2O
107
              CH_2O + O
                                    \rightarrow CHO + OH
108
              HCO + O_2
                                    \rightarrow CO + HO_2
109
               H_2 + OH
                                    \rightarrow H_2O + H
110
             CH_2O + Cl
                                    \rightarrow CHO + HCl
111
            CH_4 + O(^1D)
                                    \rightarrow CH_2O + H_2
112
            CH_2O + rain
113
          CH_3OOH + rain
                                    \rightarrow
114
            CH_3O_2 + ClO
                                    \rightarrow CH_3O + Cl + O_2
115
          CH_3OOH + OH
                                    \rightarrow CH_2O + OH + H_2O
120
                Br + O_3
                                    \rightarrow BrO + O_2
121
               BrO + O
                                    \rightarrow Br + O_2
123
              BrO + NO
                                    \rightarrow Br + NO_2
124
              BrO + OH
                                    \rightarrow Br + HO_2
                                    \rightarrow Br + OClO
125
             BrO + ClO
             BrO + ClO
                                    \rightarrow Br + Cl + O_2
126
127
             BrO + BrO
                                    \rightarrow Br + Br + O_2
128
          BrO + NO_2 + M
                                    \rightarrow BrONO_2 + M
             BrO + HO_2
130
                                    \rightarrow HOBr + O_2
130b
             BrO + HO_2
                                    \rightarrow HBr + O_3
131
             O + HOBr
                                    \rightarrow OH + BrO
             Br + CH_2O
                                    \rightarrow HBr + CHO
134
135
              Br + HO_2
                                    \rightarrow HBr + O_2
136
             HBr + OH
                                    \rightarrow Br + H_2O
  61
             HBr + rain
                                    \rightarrow
138
         O(^{1}D) + CBrClF_{2}
                                    \rightarrow Br + Cl + COF_2 + products
           O(^1D) + CBrF_3
140
                                    \rightarrow Br + COF_2 + HF + products
                                    \rightarrow Br + products
142
            OH + CH_3Br
          O(^{1}D) + CH_{3}Br
143
                                    \rightarrow Br + products
             BrO + ClO
                                    \rightarrow BrCl + O_2
144
150
                                    \rightarrow 2HNO_3(s)
         N_2O_5(g) + H_2O(s)
151
       ClONO_2(g) + H_2O(s)
                                    \rightarrow HOCl(g) + HNO_3(s)
152
       ClONO_2(g) + HCl(s)
                                    \rightarrow 2Cl(g) + HNO_3(s)
                                    \rightarrow Cl(g) + NO_2(g) + HNO_3(s)
153
         N_2O_5(g) + HCl(s)
154
         HOCl(g) + HCl(s)
                                    \rightarrow 2Cl(g) + H_2O(s)
155
        HOBr(g) + HBr(s)
                                    \rightarrow 2Br(g) + H_2O(s)
                                    \rightarrow BrCl(g) + H_2O(s)
156
         HOBr(g) + HCl(s)
         HOCl(g) + HBr(s)
                                    \rightarrow BrCl(g) + H_2O(s)
157
158
       BrONO_2(g) + HBr(s)
                                    \rightarrow 2Br(g) + HNO_3(s)
159
       BrONO_2(g) + HCl(s)
                                    \rightarrow BrCl(g) + HNO_3(s)
                                    \rightarrow BrCl(g) + HNO_3(s)
160
       ClONO_2(g) + HBr(s)
 161
       BrONO_2(g) + H_2O(s)
                                    \rightarrow HOBr(g) + HNO_3(s)
```

```
162
                                               \rightarrow Br(g) + NO_2 + HNO_3(s)
                N_2O_5(g) + HBr(s)
      180
                  O(^1D) + COF_2
                                               \rightarrow 2HF + products
      181
                 O(^{1}D) + COFCl
                                               \rightarrow Cl + HF + products
       61
                     HF + rain
                                               \rightarrow
       J_2
                       O_2 + h\nu
                                               \rightarrow O + O
      J_{3a}
                       O_3 + h\nu
                                               \rightarrow O(^1D) + O_2
                                               \rightarrow O(^3P) + O_2
                       O_3 + h\nu
       J_3
                       NO + h\nu
                                               \rightarrow N + O
    J_{NO}
                                               \rightarrow NO + O
   J_{NO2}
                      NO_2 + h\nu
  J_{NO3a}
                      NO_3 + h\nu
                                               \rightarrow NO + O_2
                      NO_3 + h\nu
                                               \rightarrow NO_2 + O
  J_{NO3b}
  J_{N2O5}
                     N_2O_5 + h\nu
                                               \rightarrow NO_2 + NO_3
                                               \rightarrow OH + NO_2
 J_{HNO3}
                     HNO_3 + h\nu
   J_{PNA}
                   HO_2NO_2 + h\nu
                                               \rightarrow HO_2 + NO_2
                                               \rightarrow Cl + NO_3
  J_{CNIT}
                   ClONO_2 + h\nu
                     HOCl + h\nu
                                               \rightarrow OH + Cl
  J_{HOCl}
                      HCl + h\nu
    J_{HCl}
                                               \rightarrow H + Cl
  J_{Cl2O2}
                     Cl_2O_2 + h\nu
                                               \rightarrow Cl + Cl + O_2
                     OClO + h\nu
                                               \rightarrow O + ClO
  J_{OClO}
                      BrO + h\nu
                                               \rightarrow Br + O
   J_{BrO}
J_{BRNO3}
                   BrONO_2 + h\nu
                                               \rightarrow Br + NO_3
                     BrCl + h\nu
                                               \rightarrow Br + Cl
   J_{BrCl}
                     HOBr + h\nu
                                               \rightarrow Br + OH
  J_{HOBr}
                     H_2O_2 + h\nu
                                               \rightarrow 2OH
  J_{H2O2}
                      N_2O + h\nu
                                               \rightarrow N_2 + O
   J_{N2O}
                                               \rightarrow H + OH
                      H_2O + h\nu
   J_{H2O}
                      CH_4 + h\nu
                                               \rightarrow CH_3 + H
   J_{CH4}
                     CH_2O + h\nu
                                               \rightarrow CHO + H
  J_{C2OA}
                     CH_2O + h\nu
                                               \rightarrow CO + H_2
  J_{C2OB}
                  CH_3OOH + h\nu
                                               \rightarrow CH_3O + OH
  J_{MHP}
                    CH_3Cl + h\nu
                                               \rightarrow CH_3 + Cl
 J_{CH3Cl}
                  CH_3CCl_3 + h\nu
                                               \rightarrow 3Cl + products
J_{MCFM}
                    CFCl_3 + h\nu
                                               \rightarrow 3Cl + F + products
    J_{F11}
                    CF_2Cl_2 + h\nu
                                               \rightarrow 2Cl + 2F + products
    J_{F12}
                   CHF_2Cl + h\nu
                                               \rightarrow Cl + 2F + products
    J_{F22}
                    CF_3Cl_3 + h\nu
                                               \rightarrow 3Cl + 3F
   J_{F113}
                                               \rightarrow 4Cl + products
   J_{CCl4}
                     CCl_4 + h\nu
                    CH_3Br + h\nu
                                               \rightarrow CH_3 + Br
J_{CH3Br}
                                               \rightarrow Br + products
                    Cx_3Br + h\nu
  J_{F1211}
                    CF_3Br + h\nu
                                               \rightarrow Br + products
  J_{F1301}
                     COF_2 + h\nu
                                               \rightarrow 2HF + products
  J_{COF2}
 J_{COFCl}
                    COFCl + h\nu
                                               \rightarrow Cl + HF + products
```

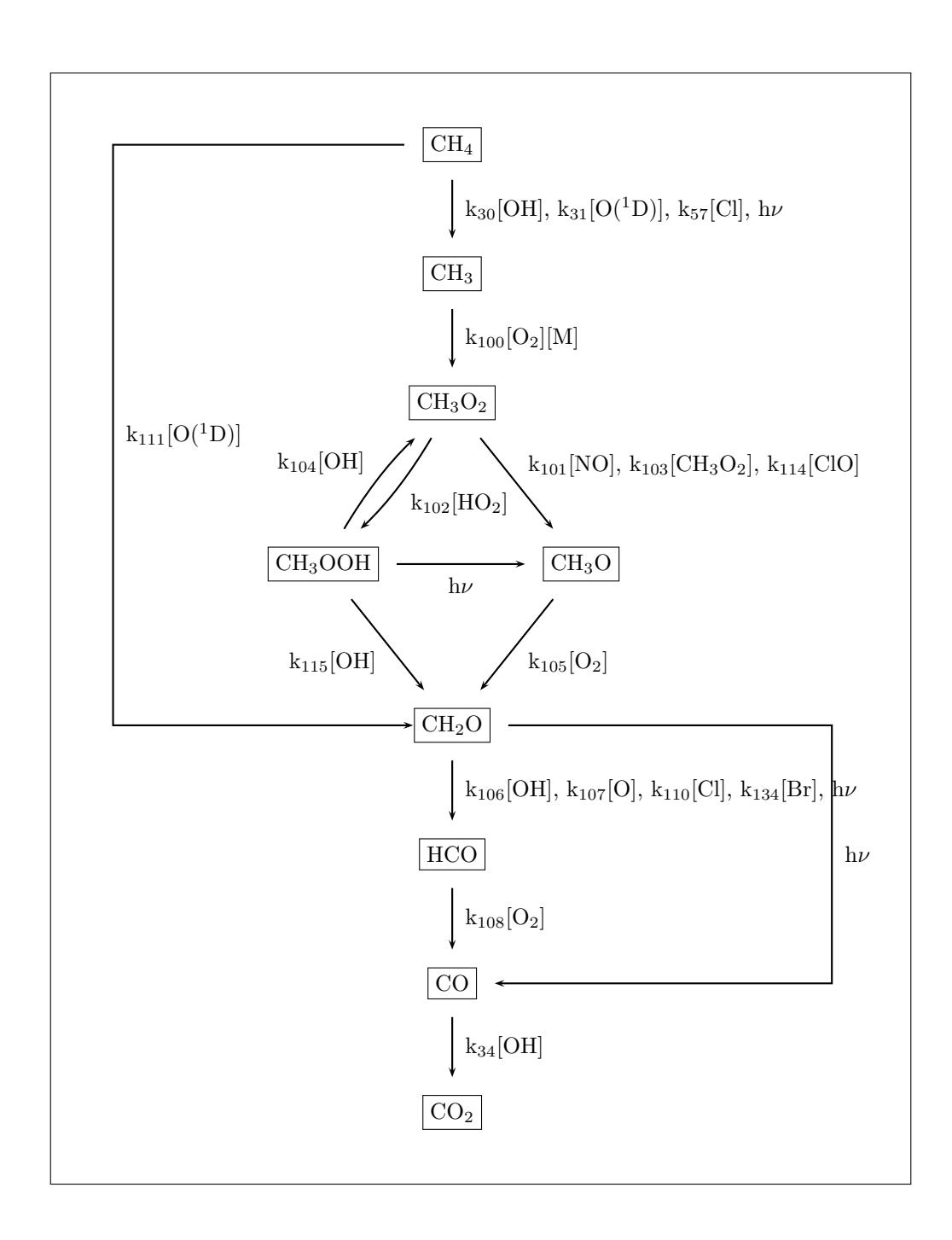
12 Appendix 2. U.S. Standard Atmosphere.

The standard profiles of temperature and O_3 in the file STDT03 are listed here. This is the default file used to set up the photolysis look-up tables.

P (hPa)	T (V)	02 ()
0.1013E+04	T (K)	03 (vmr)
	295.60	0.3082E-07
0.9161E+03	281.60	0.3082E-07
0.7153E+03	268.80	0.3144E-07
0.5517E+03	256.00	0.3641E-07
0.4199E+03	242.80	0.5097E-07
0.3147E+03	229.60	0.1044E-06
0.2327E+03	221.80	0.2388E-06
0.1709E+03	219.40	0.4084E-06
0.1251E+03	217.00	0.6852E-06
0.9139E+02	217.00	0.1268E-05
0.6677E+02	217.00	0.2100E-05
0.4882E+02	218.00	0.3021E-05
0.3577E+02	220.00	0.3985E-05
0.2628E+02	222.00	0.4897E-05
0.1937E+02	224.00	0.5464E-05
0.1431E+02	226.00	0.5866E-05
0.1061E+02	229.00	0.6358E-05
0.7899E+01	233.00	0.6831E-05
0.5912E+01	237.00	0.7234E-05
0.4449E+01	242.20	0.7184E-05
0.3368E+01	247.40	0.6774E-05
0.2566E+01	252.80	0.6049E-05
0.1965E+01	258.40	0.5465E-05
0.1514E+01	264.00	0.4609E-05
0.1172E+01	266.80	0.3685E-05
0.9088E+00	269.60	0.3011E-05
0.7058E+00	269.00	0.2314E-05
0.5469E+00	265.00	0.1861E-05
0.4221E+00	261.00	0.1527E-05
0.3242E+00	255.40	0.1302E-05
0.2476E+00	249.80	0.1096E-05
0.1879E+00	244.20	0.9237E-06
0.1417E+00	238.60	0.7866E-06
0.1062E+00	233.00	0.5897E-06
0.7901E-01	227.80	0.3627E-06
0.5839E-01	222.60	0.2879E-06
0.4292E-01	220.00	0.2950E-06
0.2400E-01	200.00	0.2444E-06
0.1040E-01	181.00	0.16E-06
0.4100E-02	181.00	0.11E-06
0.1800E-02	176.70	0.90E-07
0.7900E-03	193.00	0.80E-07
0.1900E-03	209.20	0.70E-07
0.1000E-04	230.90	0.60E-07

13 Appendix 3. CH₄ Oxidation Scheme.

The CH₄ oxidation scheme contained in the model is summarised in the following figure. The species in the thin-lined boxes (e.g. CH₃) are treated in steady state in the model.



14 Appendix 4. Cray Flowtrace.

Below is a Perfview output from the Cray J90 for the chemistry model coupled to the SLIMCAT offline transport model. The simulation analysed was for run 2 model days in a resolution of 5.6° x 5.6° (SLIMCAT parameters: LON=64, LAT=32, NIV=2, DT0=3600.0) with the SIS integration scheme. The number of chemical subtimesteps (NDDT) was 4. The most expensive subroutine is MATRIX (which inverts a matrix at grid point at each timestep). This is followed by CALCJS (which looks-up the photolysis rates) and CRATIO which contains the the iterative calculations for the partitioning of chemical families. The routine CALCJS is not very efficient in Cray terms because it simply interpolates numbers, rather tahn performing a lot of calculations. The cost of CALCJS can be reduced if not all photolysis rates are required (e.g. the experiment does not include all of the source gases). The subroutine SETTAB is expensive but it is only called at the start of the run to set up the file jtable. This cost can be avoided if jtable is saved and reused in later runs. The subroutines ADVX2 etc. are part of SLIMCAT and advect the tracers using the Prather [1986] transport scheme. The cost of chemistry is much larger than the transport.

Perftrace Statistics Report Showing Traced Routines (CPU Times are Shown in Seconds)

Name	Called	Time	Avg Tim	EX %	ACM %	Mmems	Mflops	
MATRIX	6144	6.67E+01	1.09E-02	30.1	30.1	95.4	46.7	*****
		3.78E+01						
CALCJS	3072	2.44E+01	7.95E-03	11.0	58.2	25.6	15.2	**
SETTAB	1	1.83E+01	1.83E+01	8.3	66.5	4.2	6.8	**
SETTAB ADVX2 ADVY2 SISINT	96	1.77E+01	1.85E-01	8.0	74.5	70.7	40.4	**
ADVY2	96	1.37E+01	1.42E-01	6.2	80.6	64.4	46.4	*
SISINT	6144	1.03E+01	1.67E-03	4.6	85.3	75.8	48.3	*
CALCKS	1536	6.55E+00	4.26E-03	3.0	88.2	22.5	89.2	
FINCYCL COLMOD	8	5.30E+00	6.62E-01	2.4	90.6	9.3	0.2	
COLMOD	6144	4.48E+00	7.29E-04	2.0	92.7	74.6	21.2	
CONFOR LUBKSB ACSO3W	9	2.39E+00	2.66E-01	1.1	93.7	23.0	25.4	
LUBKSB	5530	1.65E+00	2.98E-04	0.7	94.5	14.5	10.2	
ACSO3W	70015	1.61E+00	2.30E-05	0.7	95.2	1.9	3.8	
CALFLU	9	1.61E+00	1.79E-01	0.7	95.9	9.4	10.0	
CHIMIE	48	1.39E+00	2.89E-02	0.6	96.6	69.1	56.2	
		1.37E+00						
CORNEG	6144	1.26E+00	2.05E-04	0.6	97.7	111.8	68.6	
ACSSRW LUDCMP	62645	1.06E+00	1.70E-05	0.5	98.2	1.9	3.5	
LUDCMP	158	8.80E-01	5.57E-03	0.4	98.6	14.6	10.2	
INITER	48	8.48E-01	1.77E-02	0.4	99.0	125.2	78.5	
		5.55E-01						
ADVEC	48	5.35E-01	1.11E-02	0.2	99.5	89.5	0.0	
INIJTAB	1	2.86E-01	2.86E-01	0.1	99.6	61.5	39.0	
FINITER INIEXP	48	2.35E-01	4.89E-03	0.1	99.7	8.8	0.2	
INIEXP	1	2.00E-01	2.00E-01	0.1	99.8	14.8	2.8	
INICYCL	8	1.26E-01	1.57E-02	0.1	99.9	19.7	0.1	
		1.18E-01					0.0	
HETKEM								
ACSNO	700	2.23E-02	3.18E-05	0.0	100.0	2.9	6.6	
SLIMCAT	1	1.46E-02	1.46E-02	0.0	100.0	68.4	0.0	
SLIMCAT ACSSR CHTRON	632	1.30E-02	2.06E-05	0.0	100.0	5.6	23.8	
CHTRON	621	1.17E-02	1.88E-05	0.0	100.0	54.7	0.0	

PEQTEMP	48 1.7	79E-03	3.73E-05	0.0	100.0	3.0	8.2	
CORPOLE	9 1.3	37E-03	1.52E-04	0.0	100.0	19.8	72.0	
PDECLIN	48 1.3	34E-03	2.78E-05	0.0	100.0	2.8	7.4	
WCALEN	48 6.2	25E-04	1.30E-05	0.0	100.0	0.9	1.7	
FINEXP	1 2.4	43E-04	2.43E-04	0.0	100.0	4.5	0.0	
SCATCS	1 1.5	59E-04	1.59E-04	0.0	100.0	26.3	86.6	
CALNUM	1 7.8	84E-05	7.84E-05	0.0	100.0	5.4	22.6	
SETZEN	1 4.5	50E-05	4.50E-05	0.0	100.0	3.9	78.7	
GENGRID	1 4.1	17E-05	4.17E-05	0.0	100.0	15.8	61.4	
ACSHN03	1 3.9	95E-05	3.95E-05	0.0	100.0	19.9	76.6	
ACSMC	1 3.3	36E-05	3.36E-05	0.0	100.0	4.8	42.4	
ACSCCL4	1 3.3	34E-05	3.34E-05	0.0	100.0	4.8	42.6	
ACSN20	1 3.2	22E-05	3.22E-05	0.0	100.0	7.2	64.7	
ACSF22	1 2.9	93E-05	2.93E-05	0.0	100.0	4.4	33.3	
ACSO3	1 2.8	33E-05	2.83E-05	0.0	100.0	7.0	31.8	
QUANTO12	1 2.1	18E-05	2.18E-05	0.0	100.0	12.7	8.0	
ACSH202	1 2.1	14E-05	2.14E-05	0.0	100.0	3.1	32.9	
ACSF11	1 1.9	96E-05	1.96E-05	0.0	100.0	6.7	35.9	
ACSN205	1 1.8	37E-05	1.87E-05	0.0	100.0	4.5	31.7	
ACSF12	1 1.7	76E-05	1.76E-05	0.0	100.0	7.2	38.5	
ACSCNIT	1 1.3	34E-05	1.34E-05	0.0	100.0	21.6	26.3	
INICSTE	1 1.2	28E-05	1.28E-05	0.0	100.0	2.7	3.2	
ACSNO2	1 1.0	03E-05	1.03E-05	0.0	100.0	9.9	6.2	
========				=====		=====	=====	:=:

Totals 194813 2.21E+02 100.0 100.0 65.8 48.4

Whole Program

This program achieved 48.4 million floating-point operations per second during its execution.

This program appears to be a partially vectorized code.

This program showed a computational intensity of 0.73. Computational intensity is the ratio of flops to memory references. This value is considered to be moderate, indicating an algorithm with mid-range efficiency.

Routine MATRIX [Rank:1]

This routine was responsible for 30.1% of the total program CPU time. This is a significant percentage of the whole program.

This routine achieved 46.7 million floating-point operations per second during its execution.

This routine appears to be a partially vectorized code.

This routine showed a computational intensity of 0.49. Computational intensity is the ratio of flops to memory references. This value may indicate a low algorithm efficiency.

Routine CRATIO [Rank:2]

This routine was responsible for 17.1% of the total program CPU time. This routine achieved 107.1 million floating-point operations per second during its execution.

This routine appears to be an efficient vectorized code.

This routine showed a computational intensity of 1.21. Computational intensity is the ratio of flops to memory references. This value is considered to be moderate, indicating an algorithm with mid-range efficiency.

Routine CALCJS [Rank:3]

This routine was responsible for 11.0% of the total program CPU time. This routine achieved 15.2 million floating-point operations per second during its execution.

This routine appears to be a scalar code.

This routine showed a computational intensity of 0.59. Computational intensity is the ratio of flops to memory references. This value may indicate a low algorithm efficiency.

Routine SETTAB [Rank:4]

This routine was responsible for 8.3% of the total program CPU time. This routine achieved 6.8 million floating-point operations per second during its execution.

This routine appears to be a scalar code.

This is confirmed by a high instruction per flop ratio (3.8).

This routine showed a computational intensity of 1.60. Computational intensity is the ratio of flops to memory references. This value is considered to be very good, indicating an efficient algorithm.

Below is an identical experiment but using the UGAMP integration scheme (IINT=2 and NRSTEPS=12). This simulation took 267s (including Perfview overhead) compared to 221s for the SIS scheme above. For the current chemical scheme the SIS scheme is therefore cheaper as 12 is a lower limit for the iterations needed in the UGAMP scheme. If the SIS matrix were larger (currently 17x17) then the UGAMP scheme could become more favourable.

Perftrace Statistics Report Showing Traced Routines (CPU Times are Shown in Seconds)

Name								
DERIVS CRATIO JACOBI CALCJS SETTAB ADVX2 ADVY2 ODEIMP CALCKS FINCYCL COLMOD CONFOR LUBKSB ACSO3W CALFLU CHIMIE INISIS CORNEG ACSSRW INITER LUDCMP DOZONEDT ADVEC INIJTAB FINITER INIEXP INICYCL INVERT HETKEM ACSNO	79872	7.97E+01	9.98E-04	29.9	29.9	84.3	64.6	*****
CRATIO	6144	3.86E+01	6.27E-03	14.5	44.3	87.2	105.2	***
JACOBI	79872	2.51E+01	3.14E-04	9.4	53.7	112.8	100.2	**
CALCJS	3072	2.49E+01	8.11E-03	9.3	63.1	25.1	14.9	**
SETTAB	1	1.87E+01	1.87E+01	7.0	70.1	4.1	6.6	*
ADVX2	96	1.81E+01	1.89E-01	6.8	76.9	69.1	39.5	*
ADVY2	96	1.40E+01	1.46E-01	5.3	82.1	62.8	45.3	*
ODEIMP	6144	1.38E+01	2.25E-03	5.2	87.3	68.4	123.8	*
CALCKS	1536	6.59E+00	4.29E-03	2.5	89.8	22.3	88.6	
FINCYCL	8	5.41E+00	6.76E-01	2.0	91.8	9.1	0.2	
COLMOD	6144	5.29E+00	8.61E-04	2.0	93.8	75.8	17.9	
CONFOR	9	2.43E+00	2.70E-01	0.9	94.7	22.6	25.0	
LUBKSB	5530	1.64E+00	2.96E-04	0.6	95.3	14.6	10.2	
ACS03W	70015	1.63E+00	2.32E-05	0.6	95.9	1.9	3.8	
CALFLU	9	1.62E+00	1.80E-01	0.6	96.6	9.3	9.9	
CHIMIE	48	1.41E+00	2.94E-02	0.5	97.1	67.9	55.2	
INISIS	6144	1.36E+00	2.21E-04	0.5	97.6	104.9	87.9	
CORNEG	6144	1.29E+00	2.11E-04	0.5	98.1	109.0	66.9	
ACSSRW	62645	1.14E+00	1.82E-05	0.4	98.5	1.8	3.2	
INITER	48	8.94E-01	1.86E-02	0.3	98.8	118.7	74.5	
LUDCMP	158	8.74E-01	5.53E-03	0.3	99.2	14.7	10.3	
DOZONEDT	6144	5.67E-01	9.24E-05	0.2	99.4	63.9	84.5	
ADVEC	48	5.36E-01	1.12E-02	0.2	99.6	89.3	0.0	
INIJTAB	1	2.76E-01	2.76E-01	0.1	99.7	63.7	40.4	
FINITER	48	2.37E-01	4.93E-03	0.1	99.8	8.7	0.2	
INIEXP	1	2.05E-01	2.05E-01	0.1	99.8	14.4	2.7	
INICYCL	8	1.28E-01	1.60E-02	0.0	99.9	19.4	0.1	
INVERT	158	1.12E-01	7.10E-04	0.0	99.9	10.8	0.0	
HETKEM	6144	1.02E-01	1.66E-05	0.0	100.0	31.6	0.0	
ACSNO	700	2.25E-02	3.21E-05	0.0	100.0	2.9	6.5	
ACSNO SLIMCAT ACSSR	1	1.48E-02	1.48E-02	0.0	100.0	67.5	0.0	
ACSSR	632	1.25E-02	1.98E-05	0.0	100.0	5.9	24.8	
CHTRON	621	1 19E-02	1 91E-05	0 0	100 0	53.8	0 0	
PEQTEMP PDECLIN	48	1.85E-03	3.84E-05	0.0	100.0	2.9	7.9	
PDECLIN	48	1.40E-03	2.91E-05	0.0	100.0	2.7	7.0	
CORPOLE	9	1.38E-03	1.53E-04	0.0	100.0	19.6	71.4	
WCALEN	48	6.39E-04	1.33E-05	0.0	100.0	0.9	1.7	
FINEXP	1	2.46E-04	2.46E-04		100.0		0.0	
SCATCS	1	1.65E-04	1.65E-04	0.0	100.0	25.3	83.3	
CALNUM	1	7.90E-05	7.90E-05	0.0	100.0	5.3	22.4	
SETZEN	1	4.41E-05	4.41E-05		100.0	4.0		
GENGRID	1	4.23E-05	4.23E-05		100.0		60.5	
ACSHN03	1	3.82E-05	3.82E-05		100.0	20.6		
ACSCCL4	1	3.19E-05	3.19E-05		100.0	5.0	44.5	
ACSN20		3.17E-05			100.0	7.3	65.7	
ACSMC		3.17E-05			100.0	5.0	44.8	
ACSF22		2.94E-05			100.0	4.4		
ACSO3		2.81E-05			100.0	7.1		
QUANTO12		2.11E-05			100.0		8.2	
ACSH202	1	2.08E-05	2.08E-05	0.0	100.0	3.2	33.9	

ACSN205	1 1.80E-05 1.80E-05	0.0 100.0	4.7	33.0	
ACSF11	1 1.76E-05 1.76E-05	0.0 100.0	7.4	39.9	
ACSF12	1 1.71E-05 1.71E-05	0.0 100.0	7.4	39.7	
INICSTE	1 1.52E-05 1.52E-05	0.0 100.0	2.3	2.7	
ACSCNIT	1 1.33E-05 1.33E-05	0.0 100.0	21.7	26.4	
ACSNO2	1 1.01E-05 1.01E-05	0.0 100.0	10.1	6.3	
=======	=======================================		=====		=======================================
Totals	348413 2.67E+02	100.0 100.0	67.5	61.8	

Routine DERIVS

[Rank:1]

This routine was responsible for 29.9% of the total program CPU time. This is a significant percentage of the whole program. This routine achieved 64.6 million floating-point operations per second during its execution.

This routine appears to be a partially vectorized code.

This routine showed a computational intensity of 0.77. Computational intensity is the ratio of flops to memory references. This value is considered to be moderate, indicating an algorithm with mid-range efficiency.

Routine CRATIO [Rank:2]

This routine was responsible for 14.5% of the total program CPU time. This routine achieved 105.2 million floating-point operations per second during its execution.

This routine appears to be an efficient vectorized code.

This routine showed a computational intensity of 1.21. Computational intensity is the ratio of flops to memory references. This value is considered to be moderate, indicating an algorithm with mid-range efficiency.

Routine JACOBI

[Rank:3]

This routine was responsible for 9.4% of the total program CPU time. This routine achieved 100.2 million floating-point operations

per second during its execution.

This routine appears to be an efficient vectorized code.

This routine showed a computational intensity of 0.89. Computational intensity is the ratio of flops to memory references. This value is considered to be moderate, indicating an algorithm with mid-range efficiency.

Routine CALCJS [Rank:4]

This routine was responsible for 9.3% of the total program CPU time. This routine achieved 14.9 million floating-point operations per second during its execution.

This routine appears to be a scalar code.

This routine showed a computational intensity of 0.59. Computational intensity is the ratio of flops to memory references. This value may indicate a low algorithm efficiency.